Received: 22 January 2021 | Revised: 19 May 2021 | Accepted: 19 May 2021

DOI: 10.1111/apha.13694

REGULAR PAPER

ACTA PHYSIOLOGICA

TRPV3 and TRPV4 as candidate proteins for intestinal ammonium absorption

David Manneck[1] | **Hannah-Sophie Braun**[2] | **Katharina T. Schrapers**[2] | **Friederike Stumpff**[1]

[1]Institute of Veterinary Physiology, Freie Universität Berlin, Berlin, Germany

[2]PerformaNat GmbH, Berlin, Germany

Correspondence
Friederike Stumpff, Institute of Veterinary Physiology, Freie Universität Berlin, Oertzenweg 19b, Berlin 14163, Germany.
Email: stumpff@zedat.fu-berlin.de

Funding information
Akademie für Tiergesundheit; Deutsche Forschungsgemeinschaft, Grant/Award Number: DFG-STU 258/7-1

Abstract

Aim: Absorption of ammonia from the gut has consequences that range from encephalitis in hepatic disease to global climate change induced by nitrogenous excretions from livestock. Since patch clamp data show that certain members of the transient receptor potential (TRP) family are permeable to NH_4^+, participation in ammonium efflux was investigated.

Methods: Digesta, mucosa and muscular samples from stomach, duodenum, jejunum, ileum, caecum and colon of pigs were analysed via colourimetry, qPCR, Western blot, immunohistochemistry and Ussing chambers.

Results: qPCR data show high duodenal expression of TRPV6. TRPM6 was highest in jejunum and colon, with expression of TRPM7 ubiquitous. TRPM8 and TRPV1 were below detection. TRPV2 was highest in the jejunum but almost non-detectable in the colon. TRPV4 was ubiquitously expressed by mucosal and muscular layers. TRPV3 mRNA was only found in the mucosa of the caecum and colon, organs in which NH_4^+ was highest (>7 mmol·L^{-1}). Immunohistochemically, an apical expression of TRPV3 and TRPV4 could be detected in all tissues, with effects of 2-APB and GSK106790A supporting functional expression. In symmetrical NaCl Ringer, removal of mucosal Ca^{2+} and Mg^{2+} increased colonic short circuit current (I_{sc}) and conductance (G_t) by 0.18 ± 0.06 µeq·cm^{-2}·h^{-1} and 4.70 ± 0.85 mS·cm^{-2} ($P < .05$, N/n = 4/17). Application of mucosal NH_4Cl led to dose-dependent and divalent-sensitive increases in G_t and I_{sc}, with effects highest in the caecum and colon.

Conclusion: We propose that TRP channels contribute to the intestinal transport of ammonium, with TRPV3 and TRPV4 promising candidate proteins. Pharmacological regulation may be possible.

KEYWORDS

ammonium, colon, gastrointestinal transport, TRP channel, TRPV3, TRPV4

See editorial article: Diener M. 2021. How to manage N-waste in the intestine? *Acta Physiol* (Oxf). e13711.

1 | INTRODUCTION

Transient receptor potential (TRP) channels are expressed throughout the gastrointestinal tract where they play multiple roles that are incompletely understood.[1,2] Perhaps owing to the fact that the first member of the family to be discovered is central to phototransduction in drosophila flies,[3] the major focus of attention has so far mostly been on the role of these proteins as molecular sensors for various stimuli. Importantly, certain members of the family can be gated by heat (eg TRPV1 or TRPV3) or cold (TRPA1 or TRPM8).[4] Furthermore, the channels are modulated by a plethora of chemical stimuli including fragrant mono- and diterpenes found naturally in plants,[5] by hormones, by pH or osmolarity.[1,2,6,7] In the gastrointestinal tract, stimuli generally activate channels on submucosal neurons, leading to influx of Ca^{2+} with initiation of signalling cascades that lead both to central sensory perception or local responses. Thus, the stimulation of TRPA1 expressed by neuronal fibres of the enteric nervous system is thought to play a role in inflammatory responses with secretion of signalling molecules associated with hypersensitivity and pain as in inflammatory bowel disease.[8] On the other hand, the interaction of cinnamaldehyde with the same channel triggers motility and secretion enhancing the digestive response while simultaneously contributing to the enjoyment of food.[9]

However, TRP channels are not only expressed by enteric neurons or sensory cells, but also by cells of the transporting epithelium. Thus, a role for apical TRPA1 channels has been proposed in the mediation of prostaglandin signalling leading to anion secretion.[10-12] So far, a direct role in cation absorption has only emerged for TRPV5 and TRPV6 as major pathways mediating the uptake of Ca^{2+} by the intestine and the kidney, and for TRPM6 as the epithelial Mg^{2+} channel, with a more ubiquitous role in cellular Mg^{2+} homeostasis played by TRPM7.[13]

There are some indications that further channels from the TRP family may be directly involved in the transport of cations. Our own interest in TRP channels was triggered when searching for candidate genes that mediate the uptake of cations from the forestomach of cattle and sheep. Having evolved from the oesophagus, forestomach epithelia show marked differences to those found in monogastric species. For example, all attempts to demonstrate the expression of classical epithelial calcium channels TRPV5 or TRPV6 in sheep or cattle rumen were futile,[14,15] despite the fact that over 50% of the formidable total gastrointestinal calcium absorption of these milk-producing mammals occurs via the forestomachs.[16,17] Another striking difference is that Na^+ transport across the rumen cannot be stimulated by aldosterone in vivo,[18] while in vitro, the micromolar concentrations of amiloride used to block electrogenic uptake of Na^+ via epithelial sodium channels (ENaC) are ineffective.[19] A similar lack of amiloride-sensitive ENaC channels has been described in the caecum of rabbits and rats,[20,21] in the colon of Xenopus frogs[22] and the omasum.[23] Instead, all of these tissues express non-selective channels for the transcellular uptake of Na^+ and other monovalent cations.[20,22,24,25] A characteristic feature of these conductances is their block by divalent cations.[26-28] In the case of the ruminal epithelium, considerable evidence points towards the involvement of TRPV3 channels, with participation of other TRP channels likely. The low selectivity of the pore region of TRPV3 allows permeation not only of Ca^{2+}, but also of K^+, Na^+ and other cations such as NH_4^+.[14,29,30] Given the notorious promiscuity of many members of the TRP channel family,[27] these results are not surprising.

The question thus naturally arises whether TRP channels expressed by epithelia of monogastric species might also play a role in the uptake of cations in general, and of the much-neglected metabolite NH_4^+ in particular. Large quantities of NH_4^+ are produced from fermentational and enzymatic degradation of nitrogenous compounds in the intestinal tract of humans or farm animals.[31,32] In principle, this NH_4^+ can be utilized by microbiota for the formation of protein that can either be utilized by the host directly or re-enter the food chain after excretion. In practice, large quantities of toxic NH_4^+ are absorbed and have to be detoxified by the liver, requiring copious amounts of energy. The major product is urea, which cannot be broken up by mammalian enzymes so that large quantities must be renally excreted. Excreted urea is then rapidly degraded to nitrogenous compounds that drive both eutrophication of surface waters and global warming.[32] In livestock, the absorption of NH_4^+ from the gut thus leads to a dramatic waste of protein and energy with an environmental fall-out that can only be considered as catastrophic. In human patients with hepatic disease, absorption of ammonia into blood contributes to encephalopathy with ultimately lethal consequences.[33]

Classically, uptake of ammonia from the gut was thought to occur via simple diffusion of the uncharged form, NH_3, across the lipid membrane surrounding the cell.[34] However, NH_3 is in fact a highly polar molecule, and lipid diffusion does not play a major role in transport across biological preparations. Instead, a role for AMT/Rh proteins[35] and aquaporins[36] has clearly emerged. Current models suggest that these proteins catalyse the deprotonation of NH_4^+, allowing NH_3 to permeate a protein pore,[35,37,38] resulting in a rapid and pH-independent net uptake of NH_3 via an electroneutral process, leading to cytosolic alkalinization. Apart from this pathway, in some preparations, there is clear evidence supporting electrogenic uptake primarily in the protonated form as NH_4^+ with acidification of the cytosol. This may involve bona fide K^+-channels,[39] but also non-selective cation channels, as has repeatedly been shown for Xenopus oocytes,[30,40] but also for epithelia from the rumen.[14,31] There is also evidence for

an electrogenic uptake pathway for NH_4^+ by the caecum of pigs.[41] The low selectivity of many TRPV channels[27] makes them prime candidates for the permeation of NH_4^+, as has been directly shown for the bovine TRPV3 via patch clamp measurements.[29,30]

Despite the importance of the pig both as a farm animal and as an experimental model for humans, very little is currently known about the distribution and function of TRP channels in gastrointestinal epithelia of this species and almost nothing about the absorption of NH_4^+. Based on our previous studies of the rumen, the current study investigated the semi-quantitative distribution of mRNA encoding for a selection of TRP channels along the porcine gastrointestinal tract. In a further step, we investigated the expression of two non-selective members (TRPV3 and TRPV4) on the protein level via Western blot and immunohistochemistry. In a final step, evidence for a possible functional participation of these two candidate proteins in the transport of monovalent cations was investigated via Ussing chamber measurements.

2 | RESULTS

2.1 | PCR

To screen for the presence of selected members of the TRP channel family in the porcine gastrointestinal tract, tissues from different segments (stomach (fundus and cardia), duodenum, middle jejunum, ileum, caecum and middle colon) of 4 different pigs of ~10 weeks killed within an in-house study (subsequently referred to as "T") were examined semi-quantitatively via qPCR (Table 1). Expression was investigated both in the stripped epithelium (containing residual submucosa) and in the muscular layers of the respective sections and mRNA levels were compared to the reference genes YWHAZ, GAPDH and ACTB and scaled to the average value of the samples. Relative to these genes, significantly different expression levels were found for the various tissues (Figure 1).

Signals corresponding to mRNA for the Mg^{2+} conducting channels TRPM6 and TRPM7 were found throughout the

TABLE 1 Amplicon length and primer sequences of the target genes

Gene	Length (bp)	A_t	Primer	Accession no.
TRPV1 fwd	107	59°C	ACCTTGTTTTCTTGTTCGGCT	XM_013981216.2
TRPV1 rev			AGACAAGCCCTCGACACTTG	
TRPV2 fwd	164	59°C	CAAGTGGTACCTGCCCCTG	XM_021067918.1
TRPV2 rev			AGAGGAAGACGAGGTAGACC	
TRPV3 fwd	202	59°C	ATGCTCATTGCCCTGATGGGAGAGAC	XM_005669116.3
TRPV3 rev			ACTTCACCTCGTTGATCCGCAGACAC	
TRPV6 fwd	291	59°C	CTTCTTTGGACAGACCATCC	XM_021078898.1
TRPV6 rev			ATGATAAAGAAAGCTGAGGCA	
TRPV4 fwd	194	60°C	CGCTCTATGACCTCTCCTCC	XM_021071776.1
TRPV4 rev			GGCACACAGATAGGAGACCA	
TRPM6 fwd	214	59°C	TGTAGCTGTGAGGAACGTAT	XM_021064975.1
TRPM6 rev			GGAGAGCCTTATCCTCTTGT	
TRPM7 fwd	254	59°C	GTTTTGCCTCCACCACTTAT	XM_013993003.1
TRPM7 rev			ATCTGAATGCACATCTGCTC	
TRPM8 fwd	183	59°C	TCTCGAAAGTTCCCACCTGT	XM_021074741.1
TRPM8 rev			TCATCATTGGCTAGGTCCAGC	
ACTB fwd	127	60°C	GACATCAAGGAGAAGCTGTG	XM_003124280.5
ACTB rev			CGTTGCCGATGGTGATG	
ACTB probe			CTGGACTTCGAGCAGGAGATGGCC	
YWHAZ fwd	113	60°C	AAGAGTCATACAAAGACAGCAC	XM_021088756.1
YWHAZ rev			ATTTTCCCCTCCTTCTCCTG	
YWHAZ probe			ATCGGATACCCAAGGAGATGAAGCTGAA	
GAPDH fwd	117	60°C	CAAGAAGGTGGTGAAGCAG	NM_001206359.1
GAPDH rev			GCATCAAAAGTGGAAGAGTGAG	
GAPDH probe			TGAGGACCAGGTTGTGTCCTGTGACTTCAA	

Abbreviation: A_t, annealing temperature.

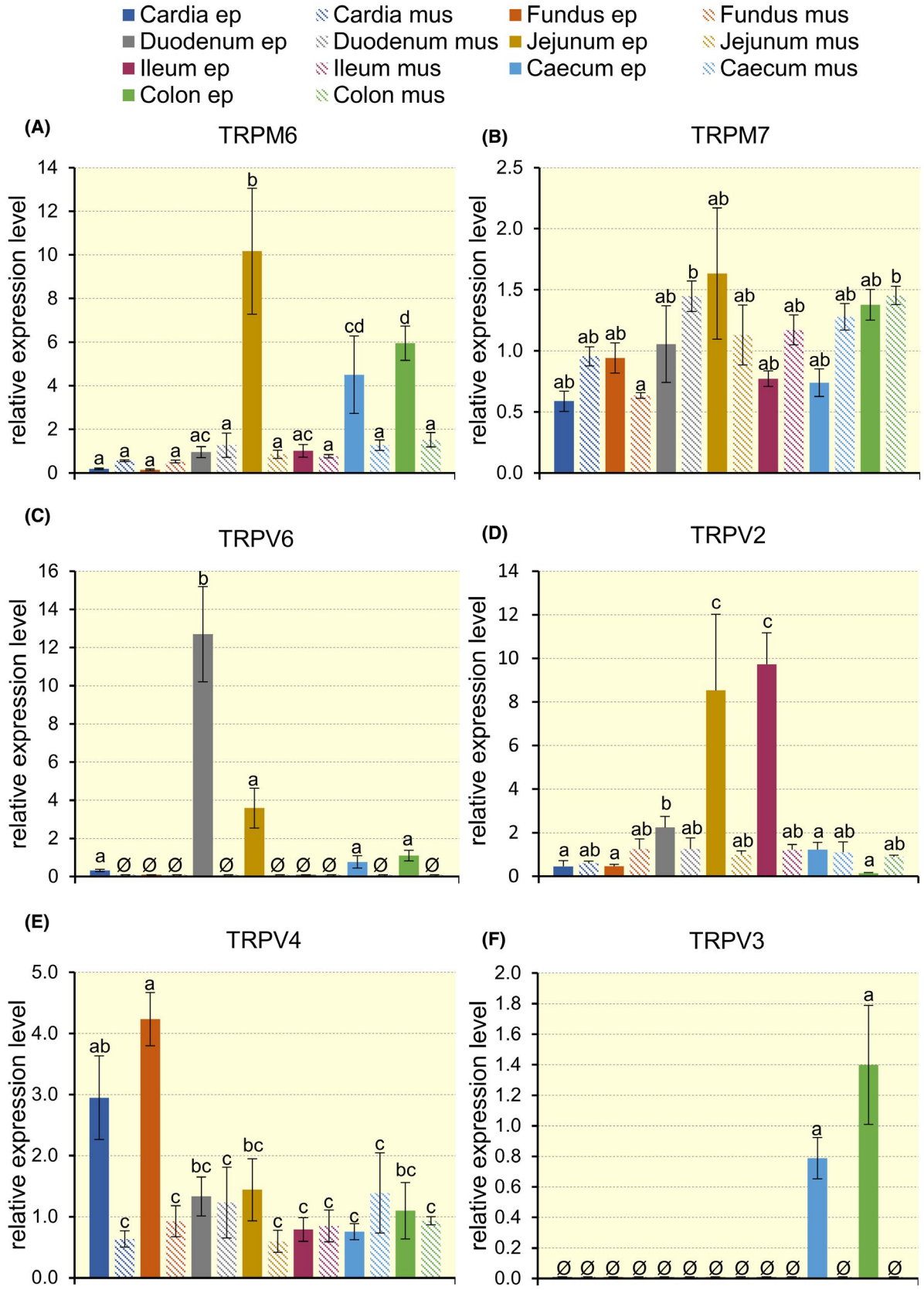

FIGURE 1 Semi-quantitative comparison of the mRNA expression of different gastrointestinal tissues (cardia and fundus of stomach, duodenum, jejunum, ileum, caecum, colon) from the stripped epithelium ("ep", containing residual submucosa) or muscle layer ("mus") of 4 pigs. The expression was normalized to the reference genes YWHAZ, GAPDH and ACTB and scaled to the average value of the samples. Bars that do not share a letter are significantly different ($P \leq .05$). Data are given as means ± SEM. Ø indicates when expression was below the detection level. TRPV1 and TRPM8 could not be detected in any segment

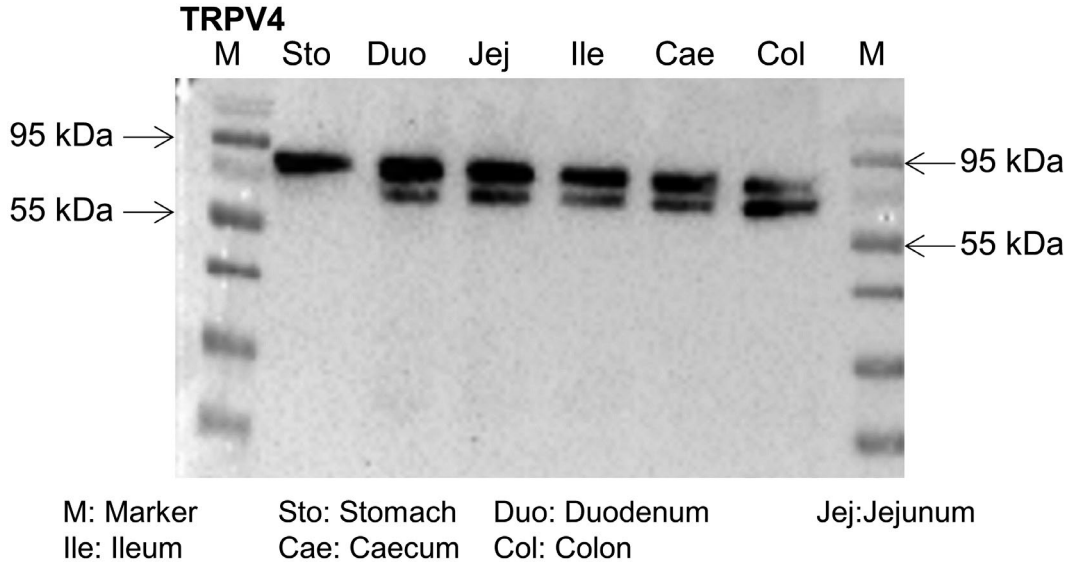

FIGURE 2 Western blot of protein from different porcine gastrointestinal tissues, stained by a TRPV4 antibody (PA5-41066). In all tissues a band at the expected level of ~90 kDa was visible. With the exception of the stomach, another band was visible at ~80 kDa

gastrointestinal tract, with expression of TRPM6 highest in the mucosal layers of the jejunum, followed by the caecum and colon (Figure 1A). Smaller amounts of TRPM6 mRNA were found in the remaining mucosa and in the muscular layers of all segments tested. Conversely, the expression of TRPM7 was high throughout and similar in muscular tissue and in the mucosa ($P = .2$; Figure 1B).

As expected, mRNA expression of TRPV6, which is a very well-established major uptake pathway for Ca^{2+} by the intestine, was highest in the duodenum. Lower levels were found in the jejunum, caecum, colon and cardia of the stomach. Interestingly, no signals for mRNA encoding for TRPV6 could be detected in ileum and fundus of the stomach or in tissue from the muscular layers (Figure 1C).

TRPV2 mRNA expression was highest in the mucosal layers of the small intestine, especially jejunum and ileum. Low mRNA expression was detected in the mucosal tissues of the stomach and caecum, as well as in the muscle layers. In the colon, signals were near the detection limit (Figure 1D).

An expression of mRNA for TRPV4 was found in both mucosal and muscular layers of all tissues studied, with the strongest expression occurring in the mucosa of the stomach (cardia and fundus; Figure 1E).

Messenger RNA encoding for TRPV3, the channel that has been proposed to serve as one pathway for the uptake of cations including NH_4^+ from the rumen,[14,29,30] could only be found in the mucosa of the caecum and colon, which are interestingly also the gastrointestinal organs with the highest levels of luminal NH_4^+ (Figure 1F and Table 2). No signals could be amplified in any of the other segments or in the muscular layers. However, it should be mentioned that the primer used in these experiments was only suitable for the amplification of the full-length 90 kDa TRPV3 protein. Apart from this long variant of TRPV3, a shorter variant of ~60 kDa has been described in mice[42] (XP_006533411.1) and in bovines[30] (AAI46079.1). We therefore designed several primers targeting segments common to both variants and which theoretically should capture them both (see Supporting Table A). Despite successful amplification by gel electrophoresis and subsequent sequencing, these 3 primers were not suitable for qPCR as they produced at least two melting curves. Only a 4th primer pair that binds to the long but not to the short variant was applicable for qPCR and produced the desired unitary melting curve. In retrospect, the failure of the other primers may indicate that mRNA of both variants might have been present in the tissue samples. The qPCR results thus suggest expression of the full-length TRPV3 mRNA sequence by caecum and colon, but neither confirm nor rule out the possibility that a further variant is expressed by these or other segments of the gastrointestinal tract.

Although control tissues tested positive (liver or medulla oblongata), no signals for TRPV1 or TRPM8 could be found in any of the porcine gastrointestinal sections in either the mucosa or the muscular layers. It should also be mentioned that despite numerous tries, we were unable to establish a porcine primer for TRPV5 that was clearly separate from TRPV6.

2.2 | Immunochemical detection of TRPV3 and TRPV4 via Western blot

In a further step, we attempted to investigate the expression of the non-selective cation channels TRPV3 and TRPV4 on the level of the protein. Since commercial antibodies for use in the porcine species are not available, we used epitope

screening to select suitable antibodies directed against a common sequence.

Staining for TRPV4 (directed against the epitope [AA 719-768]) was found in all sections at the predicted height of ~90 kDa. In all tissues but the stomach, a further band was observed at ~80 kDa that may reflect either a degradation product or a variant (Figure 2).

For staining of the porcine TRPV3, we used an antibody (ABIN863127) produced for the human, mouse and rat TRPV3 and which we previously established for use in the bovine species.[30] With the exception of a single E → V switch, the target epitope of this antibody (AA 458-474) is identical in pigs and bovines and interacts with both the large 797a (~90 kDa) and the smaller 526a (~60 kDa) variant of the bovine TRPV3 (see Supporting Table A and Ref. [30]). In porcine tissues, a weak band at 90 kDa could be detected in 2 of 9 blots of porcine colon (Figure 3A), while a stronger band at ~60 kDa was detected in all blots and all 6 intestinal sections from stomach to colon and in porcine skin (Figure 3A,B). Control samples of mouse skin showed a similar staining pattern (data not shown), in line with the reported long (NP_001357935.1) and short (XP_006533411.1) murine protein sequences. In samples with high expression, a doubling of the band could be observed, possibly reflecting degradation or phosphorylation.

2.3 | Confocal laser microscopy

To localize the expression pattern of these proteins, native tissues ("T") were stained with both TRPV3 and TRPV4 antibodies and investigated via fluorescent imaging, with

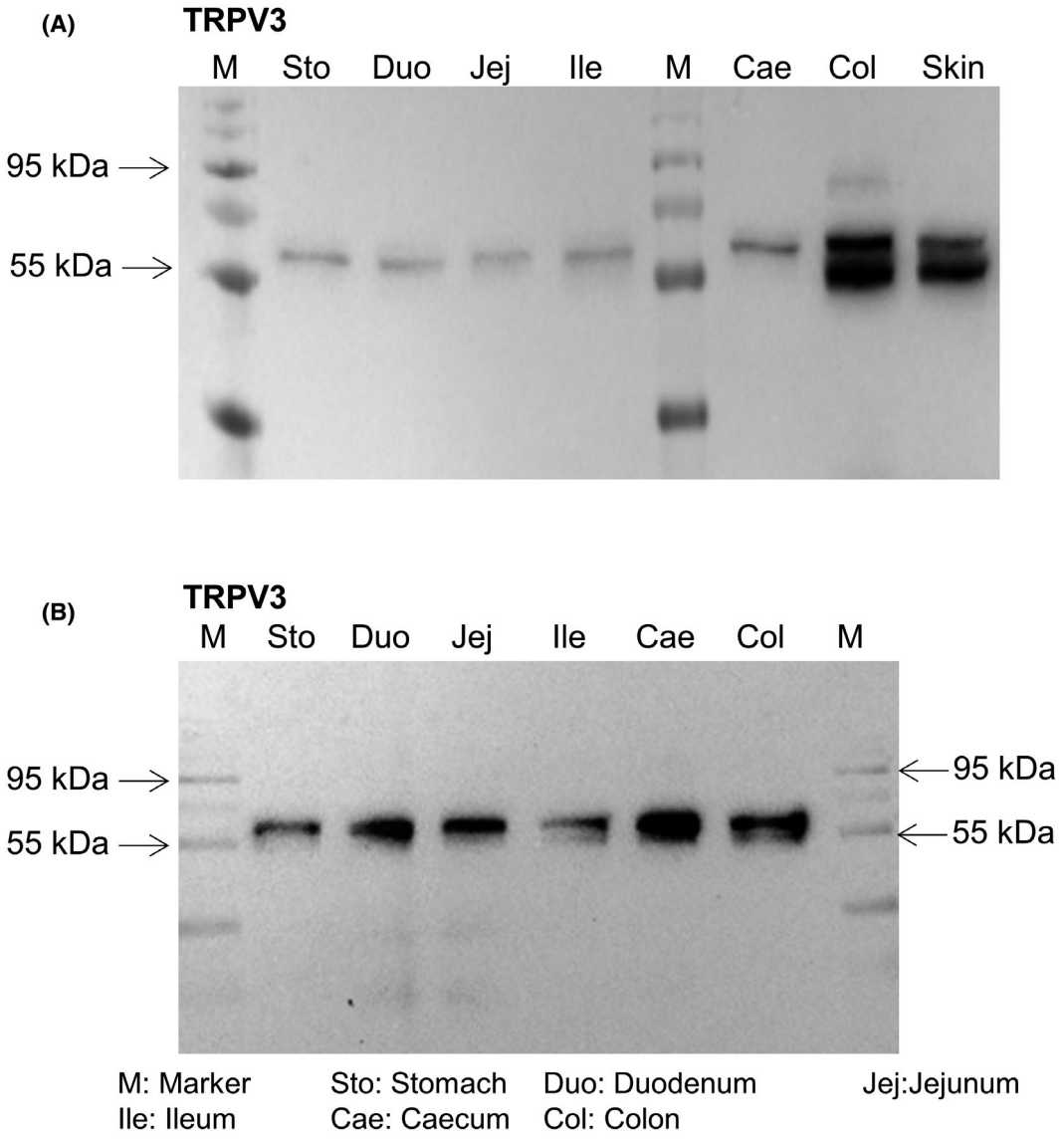

FIGURE 3 Western blot of protein from different porcine gastrointestinal tissues and from porcine skin, stained by a TRPV3 antibody (ABIN863127). A, In 2 of 9 blots a weak band at ~90 kDa was found in the colon. A and B, In all tissues a distinct band at ~60 kDa was found, sometimes doubled (see text for details)

DAPI used to mark the cell nuclei. Light settings were optimized for each preparation using standard software (ZEN, Zeiss, Jena, Germany). The same microscope settings were used to study the secondary antibody controls, which were routinely fixed onto the same slide. These controls only showed staining for DAPI. Otherwise, we made no attempt to work with fixed gain settings and the staining intensities seen in Figure 4 were optimized for each slide and do not allow a quantitative comparison of protein expression in the various segments.

In epithelia from the stomach, staining was observed along the gastric pits and in the surface epithelial cells. In the duodenum, staining of the epithelial cells was somewhat diffuse. In all more distal segments, staining was clearly strongest in the apical membrane of the cells facing the lumen (Figure 4). The staining of areas in the crypts or in the cytosol was often only subtle or not detectable.

2.4 | pH and NH_4^+ in ingesta

In order to get an overview of the physiological scenario, the ammonium concentrations and the pH of the ingesta of 4 pigs of ~10 weeks ("T") were examined in various intestinal sections, namely stomach, duodenum, middle jejunum, ileum, caecum and middle colon (Table 2). As expected, the pH value was found to rise steadily in the aboral sections of the small intestine, reflecting pancreatic secretion and chloride-bicarbonate exchange, and subsequently decreased in the fermenting sections of the caecum and colon, where resident microbiota produce short chain fatty acids from organic matter.[43,44] The ammonium concentrations remained at a relatively low level in the stomach and the small intestine, increasing substantially in the fermentative parts of the gut with microbial degradation of nitrogenous compounds.

TABLE 2 pH and ammonium content of gastrointestinal ingesta

		pH	NH_4^+ ($mmol \cdot L^{-1}$)
Tissue	**N**	**Mean ± SEM**	**Mean ± SEM**
Stomach	4	3.37 ± 0.34^a	2.78 ± 1.75^a
Duodenum	4	4.49 ± 0.51^a	1.83 ± 0.64^a
Jejunum	4	6.34 ± 0.12^b	3.13 ± 0.80^a
Ileum	4	6.39 ± 0.28^b	3.47 ± 0.66^a
Caecum	4	5.68 ± 0.13^b	7.98 ± 3.62^{ab}
Colon	4	5.92 ± 0.17^b	16.52 ± 5.47^b

Note: Values that do not share a letter in the superscript are significantly different ($P \leq .05$).

2.5 | Ussing chamber measurements

2.5.1 | Removal of mucosal Ca^{2+} and Mg^{2+}

A characteristic feature of non-selective cation channels of the TRP channel family is their negative interaction with divalent cations.[26-29] For screening purposes, we investigated the effect of a removal of divalent cations on the mucosal side of stripped intestinal mucosa ("T") in a custom-built, continuously perfused Ussing chamber, allowing artefact free solution changes.[14] Experiments were performed under symmetrical conditions with solutions containing identical amounts of NaCl on the mucosal and the serosal side (see Supporting Table B). A clear rise in I_{sc} was observed in 5 of 8 jejunal and 2 of 2 colonic epithelia tested when the divalent cations Ca^{2+} and Mg^{2+} in the mucosal standard NaCl Ringer buffer were replaced by 5 $mmol \cdot L^{-1}$ EDTA ($ØCa^{2+}$ $ØMg^{2+}$, Figure 5A), reflecting transport of Na^+ from the mucosal to the serosal side. To evaluate the isolated effect of a removal of Ca^{2+} more systematically, the effects were investigated in conventional Ussing chambers. In 17 colonic tissues from 4 different pigs ("T"), Ca^{2+} in the mucosal solution was replaced by EGTA, again resulting in a significant increase in I_{sc} by 0.18 ± 0.06 $\mu Eq \cdot cm^{-2} \cdot h^{-1}$. Simultaneously, G_t increased significantly. Control tissues that were incubated in parallel showed no response (N/n = 4/23; See Table 3).

2.5.2 | Removal of mucosal and serosal Ca^{2+}

Since a "calcium-switch" classically also opens tight junction proteins,[45] we conducted further experiments in which the buffer solution on both the serosal and the mucosal side of the epithelium was replaced by nominally Ca^{2+} free solution (Supporting Table B, "Ca^{2+} free"). As expected, a rise in G_t could again be seen, but no significant changes in I_{sc} emerged (Table 3).

2.5.3 | Effect of mucosal NH_4^+

In subsequent screening experiments ("T") in the perfused Ussing chamber, the effect of NH_4^+ on currents was tested (for solutions, see Supporting Table C). A clear and concentration-dependent increase in the I_{sc} could be observed after application of mucosal NH_4^+ in 7 of 8 tissues tested (from ileum (5), jejunum (1 of 2) and colon (1); Figure 5B). In subsequent experiments, both Ca^{2+} and Mg^{2+} were removed from the mucosal NH_4Cl solution, resulting in a rapid rise in I_{sc} with return to the original level after replacement in all tissues tested (2 from caecum, 4 from the colon and 3 from the jejunum; Figure 5C).

The effect of NH_4^+ on I_{sc} and G_t was subsequently systematically investigated in parallel in conventional Ussing chambers in different tissues from 4 pigs from a commercial slaughterhouse ("S"). After incubation in an NaCl Ringer buffer additionally containing 40 mmol·L^{-1} N-methyl-D-glucamine ($NMDG^+$), this large cation was replaced by an equimolar amount of NH_4^+ on the mucosal side of the tissue in the Ussing chamber. This intervention led to significant increases in I_{sc} and G_t in all 6 tissues of the gastrointestinal tract (Figure 6) as to be expected if ammonia is transported as NH_4^+. Note that the increase in I_{sc} could not have been caused by a swelling of cells with reduction of paracellular leak flow, since G_t also increased. Subsequently, the divalent cations in the mucosal NH_4Cl buffer were replaced by 5 mmol·L^{-1} EDTA. This resulted in a further increase in I_{sc} that was significant in all tissues. G_t rose significantly in all tissues but the jejunum and the caecum. These effects were largely reversible after washout. The changes in I_{sc} and G_t induced by the solution changes (ΔI_{sc} and ΔG_t) were numerically largest in the colon and lowest in the stomach (Table 4).

Since it appears possible that the ammonia-induced rise in I_{sc} and G_t was caused by induction of an anion conductance (eg via changes in cytosolic pH), we performed additional experiments using solutions essentially as above (Supporting Table C), but in which 110 mmol·L^{-1} chloride was replaced by gluconate. As before, the solutions were bicarbonate free. After equilibration in bilateral Na-gluconate solution, 20 mmol·L^{-1} $NMDG^+$ was replaced by an equimolar amount of NH_4^+.

In colonic preparations (N/n = 2/14, "S"), I_{sc} rose from 1.04 ± 0.18 to 2.20 ± 0.23 μeq·cm^{-2}·h^{-1} after addition of 20 mmol·L^{-1} NH_4^+ ($P < .001$), or by about half of what was observed in 40 mmol·L^{-1} NH_4Cl solution (see Figure 6). G_t rose from 14.5 ± 1.08 to 18.7 ± 2.05 mS·cm^{-2} ($P < .001$). In the jejunum (N/n = 2/14, "S"), I_{sc} rose from 0.29 ± 0.044 to 1.39 ± 0.15 μeq·cm^{-2}·h^{-1} and G_t from 16.7 ± 1.46 to 21.5 ± 2.14 mS·cm^{-2} (both $P < .001$).

Further experiments were performed using tissues from piglets ("T") in bicarbonate Ringer gassed with carbogen.[14] In both colon and jejunum, replacement of 20 mmol·L^{-1} $NMDG^+$ by NH_4^+ induced a significant rise in I_{sc} and G_t (both $P < .001$), the magnitude of which did not depend on

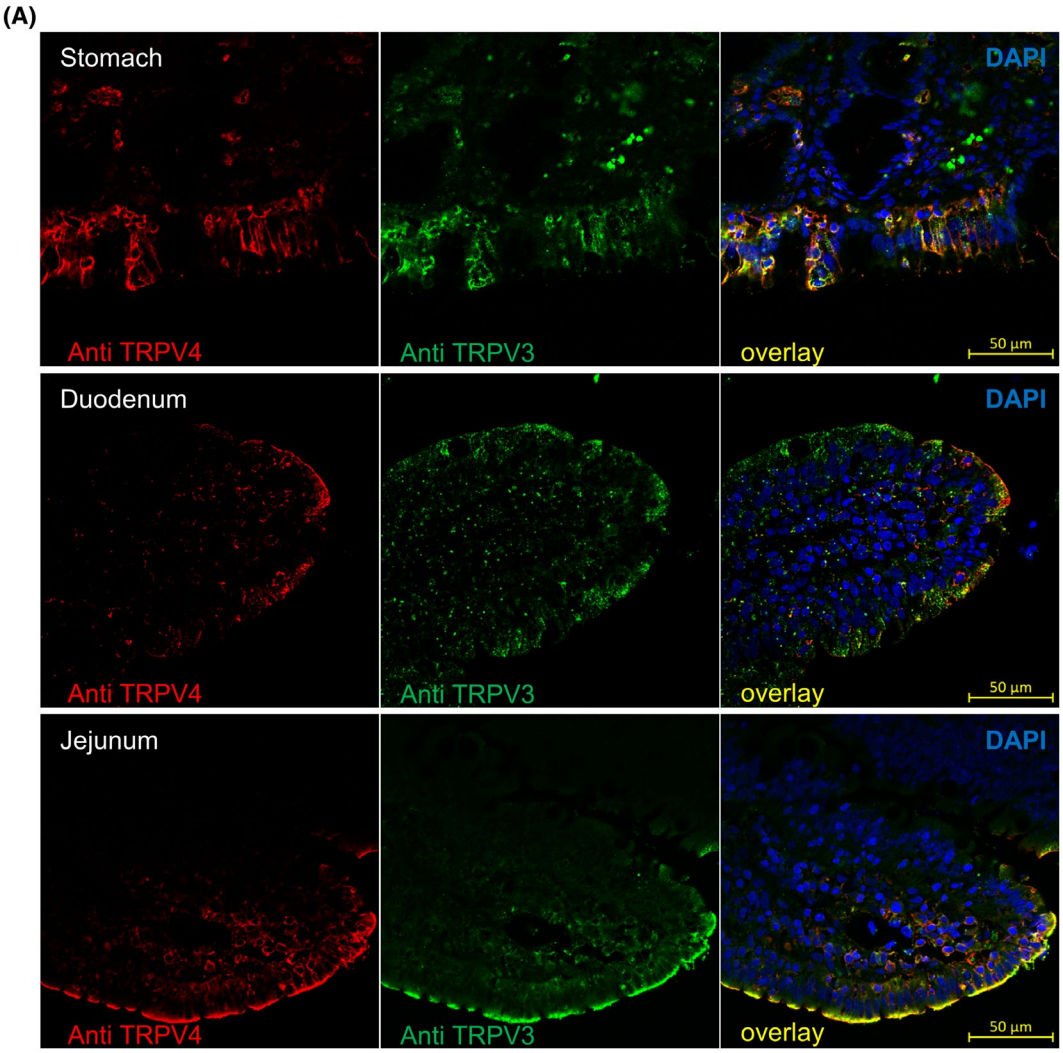

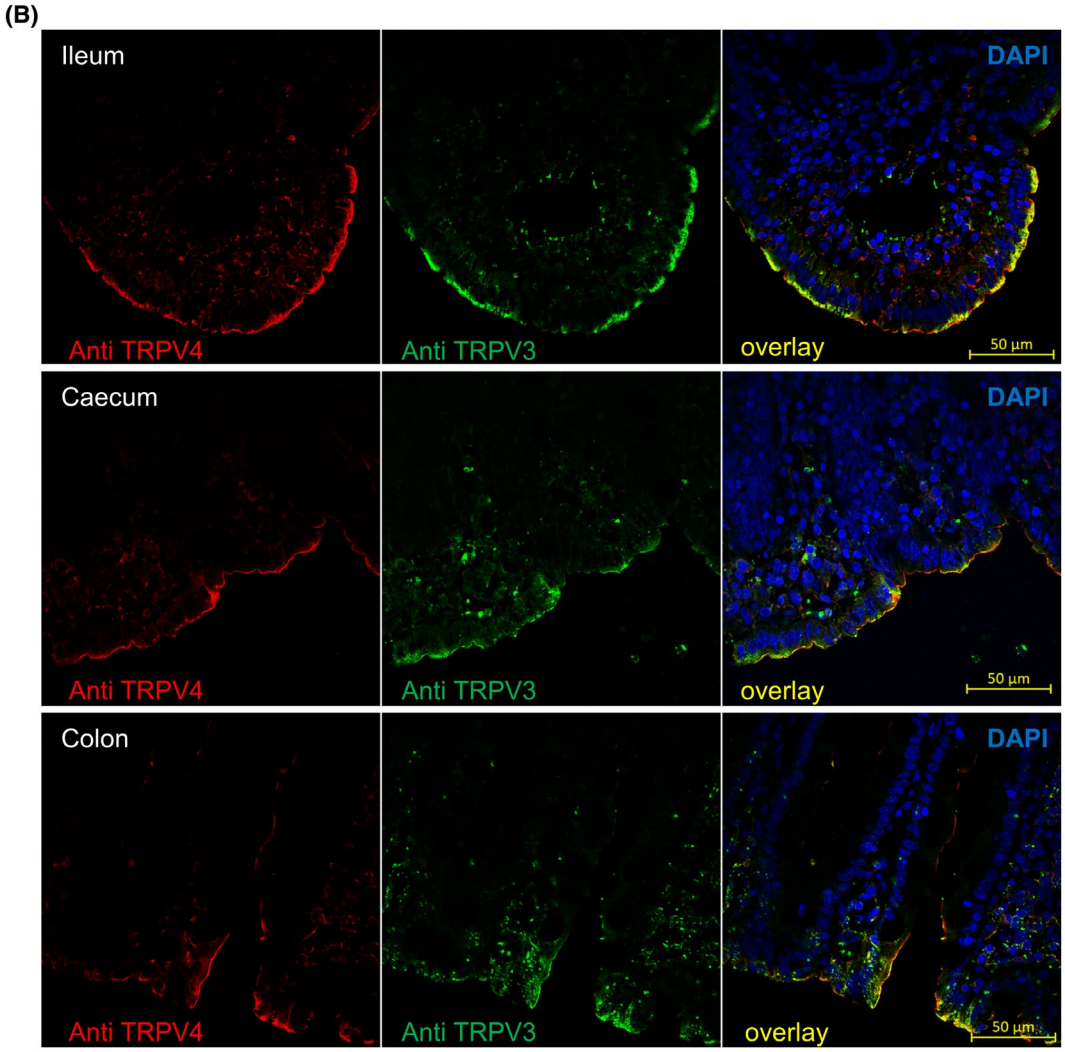

FIGURE 4 Immunohistological staining of gastrointestinal tissues of pigs using primary and secondary antibodies to mark TRPV3 (green, ABIN863127, Alexa Fluor 488) and TRPV4 (red, PA5-41066, Alexa Fluor 594). The merged pictures also show a staining for cell nuclei in blue (DAPI). A, Staining of stomach, duodenum and jejunum. The staining of TRPV3 and TRPV4 in the stomach occurred mainly in gastric pits and superficial epithelial cells. In the duodenum the staining was rather diffuse, whereas in the other tissues mainly the apical membrane was stained. Staining in the crypts was often only subtly present. B, Ileum, caecum and colon, stained as in a. Staining was most pronounced in the apical membrane

whether chloride was present (colon N/n = 3/17, jejunum N/n = 3/17) or replaced by gluconate (N/n = 3/16 and 3/18, respectively).

2.5.4 | TRP channel agonists

To test for functional involvement of TRP channels in electrogenic transport of ions across the colon, we investigated the effect of two TRP channel agonists, GSK106790A and 2-APB in Ussing chambers. A symmetrical arrangement with standard NaCl Ringer on both sides of the stripped mucosa ("T") was used (Supporting Table B). After mucosal addition, both agonists induced a steady increase in G_t over 15 minutes ($P = .004$ for GSK106790A; N/n = 3/6 versus control [Ethanol]; N/n = 3/6 and $P = .002$ for 2-APB, N/n = 3/6; Figure 7B,D). The short circuit current I_{sc} dropped rapidly in response to both agonists ($P = .009$ for GSK106790A, and $P = .002$ for 2-APB, both versus control; Figure 7A,C). The drops in I_{sc} (ΔI_{sc}) were -0.24 ± 0.06 µeq·cm^{-2}·h^{-1} (2-APB) and -0.089 ± 0.016 µeq·cm^{-2}·h^{-1} (GSK106790A), with corresponding increases in G_t (ΔG_t) of 8.56 ± 1.15 and 1.63 ± 0.44 mS·cm^{-2}.

Following the agonist-induced drop in I_{sc}, the current recovered and stabilized at a level clearly above zero after about five minutes (Figure 7). Conversely, G_t continued to rise in the 15-minute interval studied. This may mean that a paracellular pathway opened, or that a transcellular pathway opened, or, most likely, that both opened. In any case, the stabilization of I_{sc} could only occur because active, transcellular

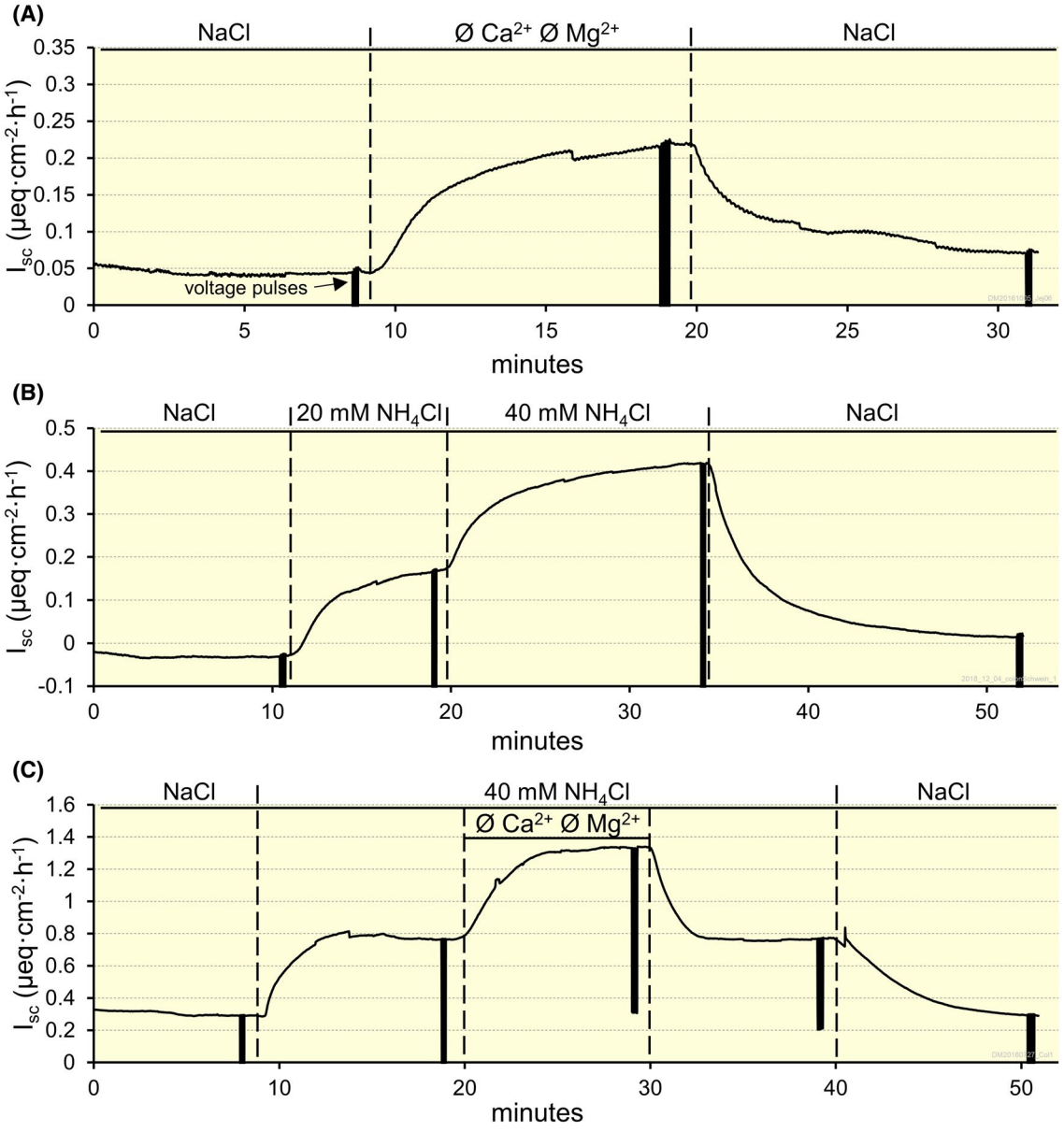

FIGURE 5 Effect of various solution changes on the mucosal side of intestinal epithelium in a modified continuously perfused Ussing chamber. The individual graphs represent original recordings from the jejunum (a) or the colon (b and c), with similar effects observed in the ileum and caecum. Before each solution change, voltage pulses were applied in order to determine epithelial conductance (vertical lines, marked with an arrow (→) in a). A, After replacing the divalent ions Ca^{2+} and Mg^{2+} with EDTA in a standard NaCl solution on the mucosal side, an immediate increase in I_{sc} could be observed. Serosally, standard NaCl Ringer solution was used. B, After the replacement of $NMDG^{+}$ by 20 or 40 mmmol·L^{-1} NH_4^{+} on the mucosal side, a distinct increase in I_{sc} could be observed. C, The change to mucosal 40 mmmol·L^{-1} NH_4^{+} increased the I_{sc}, which could be further increased by eliminating divalent ions. In all experiments the I_{sc} returned to normal values when the standard solution was used

transport increased, compensating for any loss in paracellular resistance. The simplest explanation for this is that 2-APB and GSK106790A directly opened TRP channels in the apical membrane.

3 | DISCUSSION

Despite the importance of the pig as a model for humans in biomedical research, surprisingly little is known about the expression of TRP channels by the porcine intestinal tract. This study attempted to begin to fill this gap by using qPCR to detect expression of a selection of TRP channels (TRPV6, TRPM6, TRPM7, TRPM8, TRPV2 and TRPV1) in addition to TRPV3 and TRPV4, with the expression of the latter additionally studied on the level of the protein using Western blots and immunohistochemistry. Finally, Ussing chamber measurements were utilized in order to assess the possible contributions of these channels to the transport of the monovalent cations Na^{+} and NH_4^{+}.

TABLE 3 Overview of the effect of calcium-free Ringer solutions on I_{sc} and G_t in the colon

	1. Mucosal side only Ca^{2+}-switch[a]		2. Mucosal and serosal Ca^{2+}-switch[b]		Comparison 1 vs 2
	N/n	Mean ± SEM	N/n	Mean ± SEM	*P*-value
ΔI_{sc} ($\mu eq \cdot cm^{-2} \cdot h^{-1}$)					
Ca^{2+}-switch	4/17	0.18 ± 0.06	5/14	0.008 ± 0.034	$P = .022$
Control	4/23	0.002 ± 0.012	5/29	−0.007 ± 0.009	n.s.
Switch vs control		$P = .029$		n.s.	
ΔG_t ($mS \cdot cm^{-2}$)					
Ca^{2+-}switch	4/17	4.70 ± 0.85	5/14	1.05 ± 0.35	$P < .001$
Control	4/23	−0.41 ± 0.13	5/29	−0.15 ± 0.19	n.s.
Switch vs control		$P < .001$		$P < .001$	

Note: The delta (Δ) was determined from the value immediately before the change to calcium-free Ringer to the value 15 min afterwards. Control tissues were exposed to the same standard Ringer solution throughout, although a sham solution change was performed.

[a]Mucosal solution was replaced by calcium-free Ringer with 1 $mmol \cdot L^{-1}$ EGTA.

[b]Mucosal and serosal solutions replaced by nominally calcium-free Ringer.

As mentioned, our interest in TRPV3 was sparked when searching for a candidate gene for the divalent-sensitive non-selective cation conductance of forestomach epithelia of ruminants.[23-25] Molecular biological approaches in conjunction with functional studies on native tissues, native cells and overexpressing systems confirm involvement of TRPV3 in the efflux of Na^+, NH_4^+ and Ca^{2+} from the rumen[14,29,30] with possible additional participation of other TRP channels. Similar divalent-sensitive, non-selective conductances for monovalent cations were first observed in frog and toad skin,[46,47] in the colon of Xenopus frogs[22] and in rabbit caecum.[20] Intriguingly, results of a very recent functional study of the rat caecum also point towards an involvement of non-selective TRP channels in ion transport across this segment of the gut.[21] Since the molecular identities of these divalent-sensitive conductances have remained obscure, a closer look appears merited.

Divalent cations permeate non-selective TRP channels by binding to negatively charged amino acid residues in the ion-conducting pore, which inhibits the permeation of monovalent cations with lower binding affinity (such as Na^+, Cs^+ or K^+).[27] Conversely, removal of divalent cations will result in an increase of current carried by the monovalent cation.[26-28] In line with this, a removal of divalent cations from the mucosal solution of porcine intestinal tissues incubated in Ussing chambers resulted in strong, reversible currents (Figure 5 and Table 3). Since experiments were carried out with no electrochemical gradient for NaCl present, two explanations for this rise in I_{sc} are possible: (a) an increase in current via activation of a transcellular pathway and (b) a reduction of leak backflow via tightening of the paracellular pathway. The possibility (b) can be ruled out since G_t increased significantly in all tissues studied, which is very much in line with the classical effects of a removal of Ca^{2+} on paracellular tight junction proteins.[45] Most likely, an apical cation channel opened, allowing more Na^+ to enter the cytosol and to be basolaterally driven out via the Na^+-pump. In the case of mucosal removal of divalent cations, I_{sc} increased strongly. In the case of bilateral Ca^{2+} removal, the I_{sc} did not drop despite the strong rise in G_t. In both cases, increased active transcellular transport compensated for the decrease in paracellular resistance.

In subsequent experiments, it could be shown that as in the rumen, application of mucosal NH_4^+ resulted in fully reversible, concentration-dependent and divalent-sensitive currents that tended to be highest in those compartments that physiologically have the highest concentrations of NH_4^+ (Figures 5 and 6; Tables 2 and 4).

Any involvement of chloride or bicarbonate in the NH_4^+-induced current was small since NH_4^+ induced currents of similar magnitude in gluconate solutions. However, it appears likely that pH effects contributed to the effects observed. Thus, many transport proteins, including TRPV3, are altered by changes in cytosolic pH.[48] On the other hand, the fact that the NH_4^+-induced I_{sc} could be increased by the removal of divalent cations is hardly explicable via a pH-sensitive mechanism.

It is also highly probable that the opening of tight junction proteins contributed to the rises in G_t. It appears possible that channel-like tight junctions with selectivity for NH_4^+ over Na^+ might explain the doubling of I_{sc} by replacement of as little as 20 $mmol \cdot L^{-1}$ $NMDG^+$ with NH_4^+ in a high NaCl background.[49] However, paracellular transport cannot explain the I_{sc} increase in bilateral NaCl Ringer solution after removal of divalents, which requires an active pumping mechanism. Since TRPV3 is clearly expressed by the apical membrane of the tissues studied (Figure 4), and since a divalent-sensitive permeability with $P(Na^+) < P(NH_4^+)$ has been shown directly in patch clamp experiments on cells

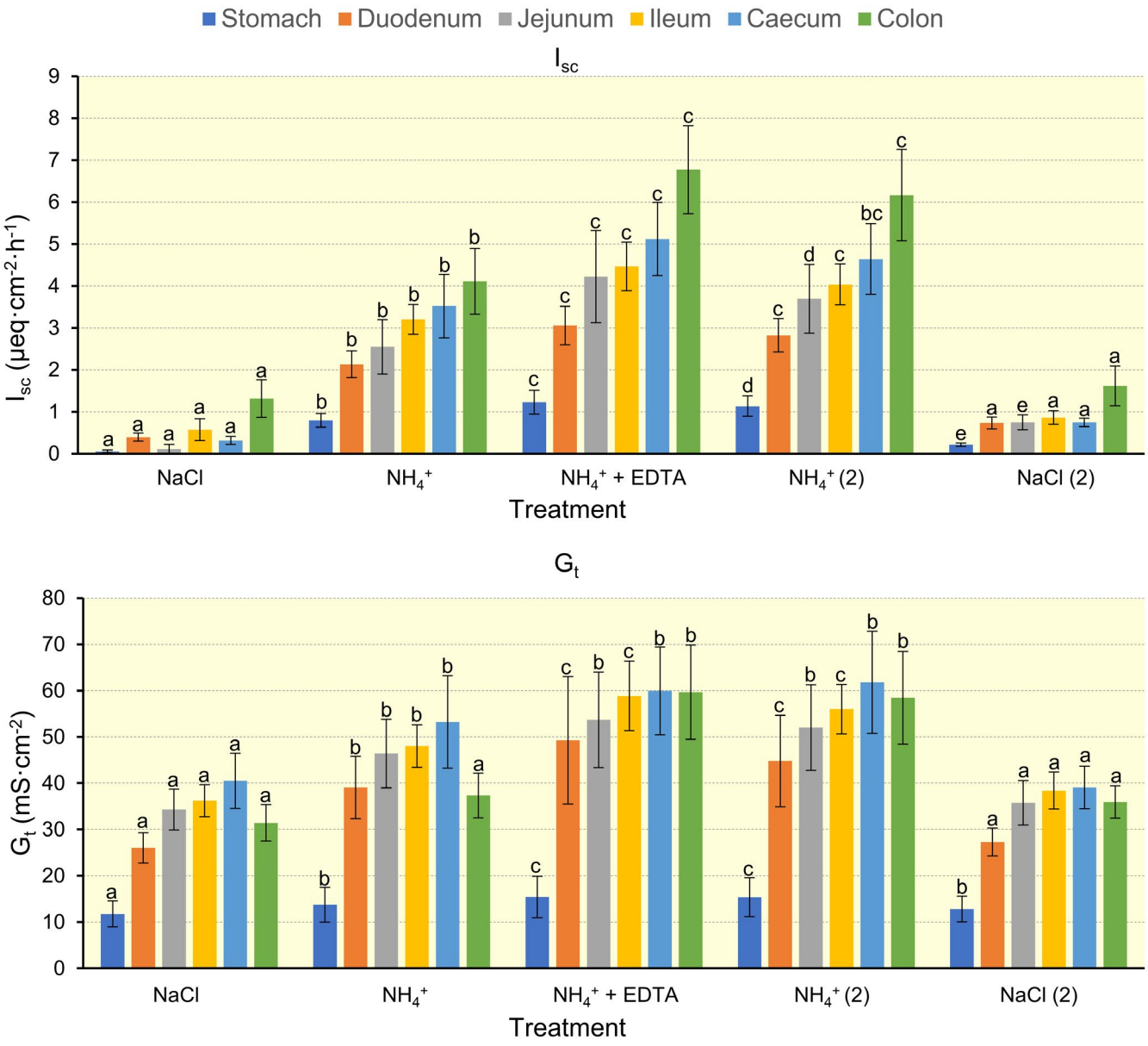

FIGURE 6 Effect of solution changes on the I_{sc} and G_t in different gastrointestinal tissues in the standard Ussing chamber. The solution change from NaCl to a 40 mmmol·L^{-1} NH_4^+ solution on the mucosal side caused an increase in I_{sc} and G_t in all tissues. After changing to a NH_4^+ solution, where Ca^{2+} and Mg^{2+} were replaced by EDTA, I_{sc} and G_t increased further. After return to the Ca^{2+} and Mg^{2+} containing NH_4^+ solution (NH_4^+ (2)) or to a NaCl (NaCl (2)) solution, a decrease to original values could be observed. Different letters indicate significant differences between solutions within a tissue type ($P \leq .05$). Data are given as means ± SEM. For differences between tissues, see Table 4

overexpressing TRPV3,[29,30] at least part of the effects should be attributable to TRPV3, with additional contributions by other pathways probable.

Functional expression of TRP channels is supported by electrophysiological effects of the TRP channel agonists GSK1016790A and 2-APB on colonic mucosa incubated in NaCl Ringer. Both agonists induced an immediate, steep drop in transepithelial resistance across the tissue that developed in the first minute after application and continued to rise (Figure 7). In contrast, the short circuit current I_{sc}, which reflects transcellular transport in this configuration, only dropped initially and then reached a new steady-state level which was clearly above zero. This means that a transcellular pathway must have been activated which eventually compensated for whatever rise in paracellular conductance continued to occur.[49]

GSK1016790A is currently thought to be selective for TRPV4. Unfortunately, there are currently no commercially available specific agonists or antagonists for TRPV3,[50] but if TRPV3 is functionally expressed, it should be activated by 2-APB. 2-APB is a classical TRP channel agonist that activates TRPV3, but also TRPV1, TRPV2 and TRPA1, but not TRPV4, TRPV5 or TRPV6,[51,52] with inhibitory effects on TRPC4, TRPC5, TRPC6, TRPM8 and TRPP1.[53] Note

TABLE 4 Overview of the changes (Δ) of I_{sc} (μeq·cm^{-2}·h^{-1}) and G_t (mS·cm^{-2}) 15 min after a solution change

ΔI_{sc} (μeq·cm^{-2}·h^{-1}) ± SEM				
	NaCl-NH_4Cl	**NH_4Cl-EDTA**	**EDTA-NH_4Cl**	**NH_4Cl-NaCl**
Tissue (N/n)	**ΔI_{sc}**	**ΔI_{sc}**	**ΔI_{sc}**	**ΔI_{sc}**
Stomach (4/8)	0.74 ± 0.18^{a}	0.43 ± 0.12^{a}	-0.09 ± 0.04^{a}	-0.92 ± 0.22^{a}
Duodenum (4/7)	1.73 ± 0.27^{ab}	0.93 ± 0.15^{ab}	-0.23 ± 0.07^{a}	-2.09 ± 0.30^{ab}
Jejunum (4/8)	2.44 ± 0.57^{ab}	1.67 ± 0.46^{ab}	-0.53 ± 0.31^{a}	-2.95 ± 0.68^{b}
Ileum (4/8)	2.63 ± 0.23^{b}	1.26 ± 0.35^{ab}	-0.43 ± 0.14^{a}	-3.17 ± 0.36^{b}
Caecum (4/8)	3.20 ± 0.68^{b}	1.60 ± 0.28^{b}	-0.48 ± 0.09^{a}	-3.9 ± 0.76^{b}
Colon (4/6)	2.80 ± 0.51^{b}	2.66 ± 0.71^{b}	-0.61 ± 0.19^{a}	-4.55 ± 0.91^{b}
ΔG_t (mS·cm^{-2}) ± SEM				
	NaCl-NH_4Cl	**NH_4Cl-EDTA**	**EDTA-NH_4Cl**	**NH_4Cl-NaCl**
Tissue (N/n)	**ΔG_t**	**ΔG_t**	**ΔG_t**	**ΔG_t**
Stomach (4/8)	2.00 ± 0.98^{a}	1.67 ± 0.73^{a}	-0.06 ± 0.33^{a}	-2.54 ± 1.55^{a}
Duodenum (4/7)	13.04 ± 5.73^{ab}	10.22 ± 7.93^{ab}	-4.51 ± 4.19^{a}	-17.50 ± 9.22^{ab}
Jejunum (4/8)	12.10 ± 3.12^{ab}	7.30 ± 3.99^{ab}	-1.71 ± 1.64^{a}	-16.25 ± 4.59^{ab}
Ileum (4/8)	11.83 ± 1.77^{b}	10.81 ± 3.96^{ab}	-2.99 ± 2.76^{a}	-17.57 ± 2.38^{b}
Caecum (4/8)	12.76 ± 4.14^{ab}	6.71 ± 2.51^{ab}	1.84 ± 2.13^{a}	-22.72 ± 7.49^{b}
Colon (4/6)	5.95 ± 2.45^{ab}	22.30 ± 9.36^{b}	-1.2 ± 1.76^{a}	-22.52 ± 6.72^{b}

Note: The first column gives ΔI_{sc} and ΔG_t after 40 mmol·L^{-1} $NMDG^+$ in an NaCl Ringer solution were replaced by an equimolar amount of NH_4^+ (NaCl-NH_4Cl). In the following column, Ca^{2+} and Mg^{2+} in the NH_4^+-solution were replaced by EDTA (NH_4Cl-EDTA). The next columns give values for a stepwise return to the original solutions (EDTA-NH_4Cl and NH_4Cl-NaCl). Different superscripts designate significant differences between tissues or within a solution (column; $P \leq .05$). The data are given as means ± SEM. For differences between solutions, see Figure 6.

that in the colon, we were unable to detect mRNA signals for TRPV1 or TRPM8, while levels for TRPV2 were almost below the detection level (Figure 1). Inhibition of TRPC4, TRPC5, TRPC6 or TRPP1 should have led to a drop in Gt, as observed in a recent study of rat caecum.[21] TRPA1, which is apically expressed by colonic epithelia,[11,12] may well have contributed to the response to 2-APB. However, TRPA1 has a high selectivity to Ca^{2+} and follows an Eisenman XI sequence with $P(Na^+) > P(K^+)$,[54] which does not predict a drop in I_{sc}. In line with this, in a recent study of the effects of the TRPA1 agonist cinnamaldehyde on porcine colon, we observed a rise in both I_{sc} and G_t.[12] These changes reflected an opening of TRPA1 with an increase in the conductance of the epithelium to cations, triggering subsequent prostaglandin-mediated secretion of anions. The latter confirms previous findings in rat colon[11] and highlights the established role of TRPA1 in cellular signalling.[8,11]

The effects in Figure 7 (decrease in I_{sc} with concomitant increase in G_t) can be understood if one assumes that 2-APB or GSK primarily activate channel(s) following an Eisenman sequence IV with $P(K^+) > P(Na^+)$, as is the case for TRPV3 and TRPV4.[26,27,30,55] Note that in our experiment, influx of Na^+ is further reduced by the high concentration of extracellular divalent cations, while efflux of K^+ can push obstructing Ca^{2+} or Mg^{2+} out of the external mouth of the pore region.[27] Accordingly, secretion of K^+ should exceed absorption of Na^+, predicting a drop in I_{sc} in conjunction with a drop in the potential across the apical membrane. The increasingly negative apical potential will enhance the driving force for Na^+, until influx of Na^+ and efflux of K^+ are equal. After a certain time, I_{sc} should reach a new steady-state equilibrium, precisely as observed (Figure 7). The rising G_t probably reflects both increases in permeation of Na^+ and K^+ through apical channels and an opening of paracellular tight junctions. On the other hand, the opening of channels may predominate since in studies of colonic or corneal cells, GSK1016790A led to a tightening of the tight junction in studies of colonic or corneal cells (with dropping G_t) and effects were visible only after 24 hours.[56,57]

In a further step, tissues from different segments of the porcine gastrointestinal tract were screened for relevant channels via qPCR. It should be mentioned in passing that establishing primers for the detection of TRP channels not just in the porcine species but also in ruminants has proved to be quite challenging.[14] In contrast to our experience with transporters such as NHE, an exceptionally high number of primers had to be tested before a primer delivered an acceptable melting curve. As emerged when attempting to establish a primer for the short variant of TRPV3, this may reflect the binding to more than one splice variant.

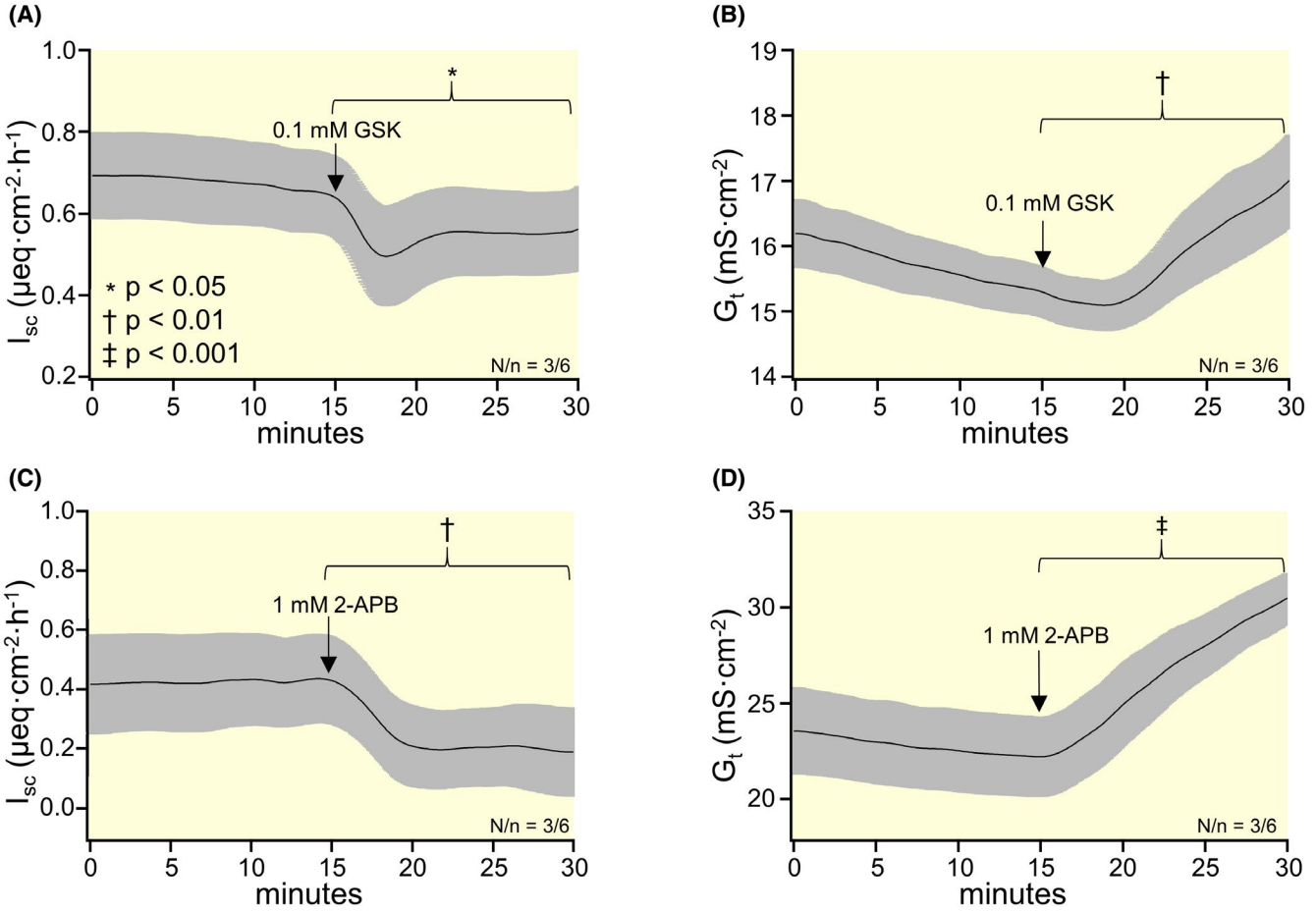

FIGURE 7 Effect of the TRP agonists 2-APB and GSK106790A (GSK) on I_{sc} and G_t in the Ussing chamber using colonic tissue of pigs. After addition of the respective agonist on the mucosal side, a decrease in I_{sc} (A and C) could be observed, while at the same time an increase in G_t occurred (B and D). Statistical comparisons were made between values taken immediately prior to addition of the agonist and after an incubation of 15 min. Data are given as means ± SEM

Our investigations started with TRP channels for which a direct role in (divalent) cation transport has been established. The expression pattern for TRPV6 confirms previously available data for the pig and other species and highlights the role of the duodenum as the major locus for Ca^{2+} absorption (Figure 1C).[16,58] Although data for the pig appear to be lacking, high mRNA expression levels of TRPM6 in the jejunum and the hindgut confirm what has been established in other species as the major locus of transcellular intestinal Mg^{2+} absorption (Figure 1A).[59-62] Interestingly, no signals for either TRPV6 or TRPM6 could be detected in samples from the muscular layers, highlighting their role in epithelial transport. Conversely, TRPM7 was found to be ubiquitously expressed by both the muscular and mucosal layers throughout the pig intestine (Figure 1B). This finding is in accordance with the proposed role of this channel in cellular Mg^{2+} homeostasis, although notably, TRPM7 may also be a primary player in epithelial Mg^{2+} uptake via formation of TRPM6/TRPM7 heteromers.[63] As mentioned, we were unable to establish a porcine primer for TRPV5 that was clearly separate from TRPV6.

In a second step, we turned to non-selective members of the TRP channel family. TRPM8 conducts both Na^+ and Ca^{2+} and is known for its activation by cool temperatures and by plant terpenoids, notably menthol and thymol.[64] We found no evidence for an expression on the level of mRNA within the porcine gastrointestinal tract (Figure 1F). Notably, mRNA for TRPM8 was also not found in the rumen[14] or in the human intestine.[65] However, expression by human colonic muscle has been reported with weaker expression within the mucosa.[66]

TRPV1 is activated by heat (>40°C), by acidic pH, and by various exogenous and endogenous substrates (eg anandamide, capsaicin).[5,26] In the murine intestine, expression was found to be highest in the intestinal nerve fibres of the colon and distal rectum.[67] Both in mice and in humans, mucosal samples from colon and rectum express TRPV1 and a role in inflammatory bowel disease has been proposed.[8,68,69] In the current qPCR study of porcine mucosa and muscularis, mRNA encoding for TRPV1 was below the threshold of detection (set at 30 cycles). This may reflect species-dependent differences, our conservative cut-off value, or the fact that samples were taken from the mid colon and not from the

distal parts, where in mouse and human samples, TRPV1 is most highly expressed. Furthermore, great care was taken to strip the epithelium from the rest of the tissue where most neurons expressing TRPV1 for neuronal signalling can be found.

TRPV2 is activated by temperatures above 52°C and is typically expressed by neurons supplying the gastrointestinal tract.[62] In the current study, mRNA encoding for TRPV2 was found in equal small amounts in the muscular layers of all segments. In the mucosal layers, TRPV2 expression was comparable to those in the muscular layers, but reached increasingly higher levels in the small intestine (Figure 1F). In the mucosal layers of the caecum, TRPV2 was low while in the colon, TRPV2 was barely detectable. Given that our samples contained small amounts of submucosa, this finding is in line with the failure to detect mRNA for TRPV2 in isolated colonic crypts of the rat.[11]

A number of studies suggest an important role for TRPV4 in the regulation of gastric motility and emptying.[70] In the colon, the channel is thought to play diverse roles in osmosensation[6,71] and regulation of barrier function,[56] with possible implications for diseases such as ulcerative colitis.[72] In the current study, the largest amount of mRNA for TRPV4 was found in the mucosa of the stomach (cardia and fundus; Figure 1D). TRPV4-encoding mRNA expression by all other porcine mucosal tissues was lower and not significantly different from the muscular layers. In Western blots stained with a rabbit antibody against TPRV4 protein, a double band at the expected height of about 90 kDa could be observed, with the doubling possibly reflecting degradation or a variant (Figure 2). A doublet of similar height has been reported in Western blot analysis of TRPV4 expression in carotid artery, kidney or skeletal muscle of wild-type mice, and disappeared in TRPV4-/- mutants.[73,74] The same antibody was used in conjunction with a secondary antibody to localize the expression of TRPV4 protein within the intact tissue via confocal laser microscopy (Figure 4). In the gastric epithelium, strong staining for TRPV4 could be observed along the gastric crypts. In intestinal epithelia, staining for TRPV4 was clearly highest in the apical membrane of cells facing the lumen of the organ. Note that the staining intensity of the different sections reflects the gain chosen for each image and not the amount of protein expressed.

TRPV3 is known to be activated by numerous stimuli, such as heat (22-40°C) or various spices (eg thymol, menthol, carvacrol).[5,75,76] The physiological function of TRPV3 is generally poorly understood[77] and research is hampered by the lack of commercially available specific agonists or blockers although the race for the development of such agents is on.[50] TRPV3 is highly expressed by the keratinocytes of the skin, where gain of function mutations are linked to a hereditary hyperkeratosis that can be so severe that joints are immobilized.[78] Very little information is available for the role of TRPV3 in the gastrointestinal tract. A role in inflammation has been suggested, although attempts to correlate clinical findings in ulcerative colitis with the expression of TRPV3 have been frustrating.[68] In what was probably the pioneering study of TRPV3 expression by the colon,[10] the authors mention "the abundant expression by the superficial absorptive cells" and suggest that functions may include epithelial ion transport. This hypothesis is supported by the functional data of this study.

Interestingly, in the current study of the porcine gastrointestinal tract, mRNA encoding for TRPV3 could only be detected in mucosa of the colon and caecum, with no signal in the muscle layer or in any other segment (Figure 1E). Similar findings have been reported for the mouse intestine, where mRNA encoding for TRPV3 could also be detected in the colon, but not in the stomach or duodenum[10] while in the rat colon, mRNA for TRPV3 was significantly higher in the crypts than in residual tissues.[11] Notably, the colon and caecum are the parts of the gut where because of fermentational degradation of amino acids and urea, concentrations of NH_4^+ are highest (Table 2). Furthermore, these tissues showed the numerically highest divalent-sensitive conductance to NH_4^+ (Figure 6, Table 4).

A note of caution is necessary since our primer was only suitable for an amplification of the mRNA of the full-length 90 kDa protein (Supporting Table A). Apart from this long variant of TRPV3, a shorter variant of ~60 kDa has been described in mice (XP_006533411.1), in human epidermal keratinocytes[42] and in bovines (AAI46079.1 and Ref. [30]). Our finding that primer pairs matching both mRNA variants all produced more than one melting curve suggests that porcine gastrointestinal tissues may also express more than one splice variant. However, this is somewhat speculative and our qPCR results confirm mRNA expression only of the long variant. Western blots stained by a mouse TRPV3 antibody showed a clearly visible band at 60 kDa in all segments and all blots studied, with a further weak band at 90 kDa observed in two blots of colonic tissues (Figure 3) and in controls of mouse skin (not shown). A similar pattern emerged in Western blots of mouse distal colon using a rabbit antibody against TRPV3,[10] in human epidermal keratinocytes using an antibody from goats[42] and in our study of the ruminal epithelium, where the same murine antibody was used as in this study.[30] It should be mentioned that in our previous study, the TRPV3 antibody was validated both in overexpressing HEK 293 cells and in Xenopus oocytes.[30]

Immunohistochemical staining of porcine tissues against TRPV3 showed expression in the gastric crypts and a clear staining of the apical membrane of the intestinal segments, with colocalization of TRPV3 and TRPV4 frequent (Figure 4). Conversely, any staining of intracellular structures was very weak. This finding is in fascinating contrast to what is typically observed in keratinocytes from skin[42,79] or

the rumen,[30] where TRPV3 antibodies typically also strongly stain the cytosolic compartment. Whatever the reasons for these differences may be, apical expression as shown here supports the involvement of TRPV3 in epithelial transport.

Under physiological conditions, the intestinal absorption of Na^+ via TRP channels will be small relative to the much larger quantities transported via the highly Na^+ selective proteins NHE and ENaC that are abundantly expressed by the colon. Instead, we suggest that as in the rumen,[29,30] one function of these poorly selective channels[27] may be to serve as one of several routes for the uptake of NH_4^+. The bovine homologue of TRPV3 has been directly shown to be permeable to NH_4^+ on the single-channel level in two different expression systems, making it a prime candidate for the divalent cation conductance reported in this study.[29,30]

It should be stressed that our findings definitely do not exclude the participation of other cation channels, including other members of the TRP channel family, in the efflux of NH_4^+ from the intestine. Furthermore, it has been shown that protein-mediated pathways for the transport of NH_3 exist.[35-37] Notably, certain types of aquaporins conduct NH_3,[36] while the colon reportedly expresses the ammonia transporters RhCG (apical) and RhBG (basolateral).[35] Although in the past, there has been some controversy surrounding the exact transport mechanism and substrate specificity of RhBG,[37] there is a broad consensus that RhCG mediates net transport of NH_3 via an electroneutral mechanism.[80] Current models suggest that all Rhesus-like glycoproteins bind NH_4^+ and catalyse the conversion to NH_3, which is then conducted through a hydrophobic pore down the concentration gradient.[37,38] Accordingly, apical expression of RhCG by the colon cannot explain the divalent-sensitive NH_4^+-induced currents observed in this study.

Further work is required to determine the basolateral efflux route (which may involve transport of NH_4^+ through K^+ channels or a coupling of RhBG [35] and pH regulating transporters such as NHE or one of the various Na^+-HCO_3^- cotransporters) and to assess the relative contributions of different pathways to total intestinal ammonia transport. However, unlike absorption in the form of the base NH_3, absorption of NH_4^+ from the colon should be very useful for the maintenance of both luminal and intracellular pH homeostasis of an organ in which protons are continuously generated in the course of the breakdown of structural carbohydrates into short-chain fatty acids.[43,44,81] Colonic pH homeostasis is essential for the survival of both the epithelium, and the microbiota living within. On the downside, ammonia has to be detoxified by the liver and the urea that is formed has to be excreted, leading to a plethora of problems that have been discussed.

In summary, we present an overview of the mRNA expression of various TRP channels along the porcine gastrointestinal tract using qPCR. The expression of two non-selective members, TRPV4 and TRPV3, was also investigated on the protein level via Western blots and confocal laser microscopy. Expression was clearly highest in the apical membrane of the intestinal segments, suggesting a function in absorption. Although further work clearly needs to be done, the functional response to an exposure to NH_4^+ containing solutions, modulated by the removal of divalent cations and the response to TRP channel agonists, suggests that a role in the transport of monovalent cations in general and NH_4^+ in particular should be considered. A concert of protein-mediated pathways for the uptake of ammonia is thus replacing older models of an uptake via the lipid membrane.[14,29,30,35-37,39] Despite their redundancy, protein-mediated uptake pathways invite new approaches concerning pharmacological modulation of ammonia losses from the hindgut, with possible implications both for limiting nitrogen losses into the environment by livestock and for the treatment of hepatic encephalopathy in humans.

4 | MATERIALS AND METHODS

4.1 | Gastrointestinal epithelium

Gastrointestinal tissues from pigs were obtained according to German guidelines of the Animal Welfare Act with approval by the local authorities (LaGeSo Reg. Nr T0264/15 and T0297/17 or from local abattoir). The pigs from T0264/15 and T0297/17 (subsequently designated as "T") consisted of a hybrid of the breeds Danbred x Piétrain at around 10 weeks of age and weighed around 25 kg. The pigs were sedated by an intramuscular injection with ketamine hydrochloride (Ursotamin, Serumwerk Bernburg AG, Bernburg, Germany) and azaperone (Stresnil, Jansen-Cilag, Neuss, Germany) and subsequently killed by intracardiac injection of tetracaine hydrochloride, mebezonium iodide and embutramide (T61, Intervet Deutschland GmbH, Unterschleissheim, Germany). Other pigs were of different ages and breeds and came from a commercial slaughterhouse ("S"). The tissue was removed approximately 10 minutes after death and was then immediately washed with PBS or Ringer solution, after which the mucosa was immediately stripped from the submucosal layers.

4.2 | PCR

Stomach (fundus and cardia), duodenum, middle jejunum, ileum, caecum and middle colon were collected from 6 pigs ("T"). After manual separation, small pieces (1 cm^2) from the muscular layers or the stripped mucosa (containing small amounts of submucosal tissue) were then immediately transferred to RNAlater (1 mL tubes; Sigma-Aldrich,

Taufkirchen, Germany) and stored overnight at 4°C, followed by storage at −80°C. For primer establishment, control tissues (liver, kidney and medulla oblongata) were additionally collected. Total RNA was isolated from all samples using a commercially available kit including DNA digestion (Nucleospin RNA ll, Macherey-Nagel, Dueren, Germany). RNA quality was checked via determination of RNA integrity (RIN) values using a lab-on-chip technique (RNA 6000 Nano, Agilent, Waldbronn, Germany). Samples from 4 pigs with the best RIN values (RIN >6.8 (ileal mucosa) or RIN > 7.3, all other tissues) were selected for further processing. 1000 ng RNA were then transcribed into cDNA (iScript cDNA synthesis Kit, Bio-Rad Laboratories, Munich, Germany) according to the manufacturer's instructions, which was diluted 1:10.

Gene-specific intron-spanning primer pairs for the porcine TRP channels and reference genes were established based on the gene sequences of the NCBI database (Table 1). In order to ensure primer specificity, amplification products of all primer pairs (Eurofins Genomics Germany GmbH, Ebersberg, Germany) were sequenced at least once and matched with the target sequence.

For the three selected reference genes, corresponding primer-probe combinations were used with FAM as the reporter and BHQ1 (ACTB) or TAMRA (GAPDH, YWHAZ) as the quencher.[82] The qPCR was performed in triplicates for 40 cycles each on a thermal cycler (Applied Biosystems/Life Technologies, Waltham, MA, USA). Negative controls (no template controls) were included. The quantification cycle (C_q) was calculated automatically by the cycler software. Dilution-series-based gene-specific amplification efficiency of all genes and expression stability of the reference genes were determined using the software qbasePLUS (Biogazelle NV, Zwijnaarde, Belgium).

Expression of mRNA levels of the target genes TRPV1, TRPV2, TRPV3, TRPV4, TRPV6, TRPM6, TRPM7 and TRPM8 was evaluated in a three-step qPCR protocol (30 s 95°C, 30 s 59°C or 60°C, 30 s 72°C) with 4 µL cDNA, 5 µL SYBR green (IQ SYBR Green Supermix, Bio-Rad Laboratories GmbH, Feldkirchen, Germany), 0.6 µL water and 0.2 µL forward and reverse primer each.

For the primer-probe combinations of the reference genes, a two-step-protocol (1 s 95°C, 20 s 60°C) was applied using 3.7 µL cDNA and iTaq Universal Probes Supermix (Bio-Rad Laboratories GmbH, Feldkirchen, Germany) in a total volume of 10 µL.

According to the software qBASEplus, ACTB, GAPDH and YWHAZ showed sufficient expression stability and were therefore used for normalization of the target genes. Normalized C_q values of the target genes were then scaled to the average value of the samples and exported as calibrated normalized relative quantity (CNRQ) values. For statistical analysis, only CNRQ values were used.

4.3 | Western blot

The tissue was cut into 1 to 2 cm² pieces after stripping and washing with PBS. The samples were then frozen in liquid nitrogen and stored at −80°C. For protein extraction the thawed sample (approx. 300 mg) was mixed with RIPA buffer (1 mL; in mmol·L^{-1}:25 HEPES, 25 NaF, 1% sodium dodecyl sulphate (SDS), 2 EDTA, protease inhibitor [cOmplete, mini, Roche, Basel, Switzerland]) and two metal spheres. The sample was then homogenized in a mixer mill (4x 1.5 min, MM 200, Retsch GmbH, Haan, Germany) and centrifuged (15 min, 15 000 g, 4°C). The supernatant was filled into a new tube and stored at −80°C after the determination of the protein concentration by the Lowry method (DC Protein Assay, Bio-Rad Laboratories GmbH, Feldkirchen, Germany). Proteins were denatured at 95°C for 5 minutes in SDS sample loading buffer. Electrophoresis with polyacrylamide gels (10%, SDS-PAGE) was performed in tris-glycine buffer (0.1% SDS) and electroblotting was done onto polyvinylidene difluoride membranes (PVDF, Immunoblot, Bio-Rad Laboratories GmbH, Munich, Germany) in tris-glycine buffer (0.037% SDS, 20% methanol, 4°C).

For the primary antibodies, dilution factors 1:500 for mTRPV3 and 1:3000 for rTRPV4 were used. The detection of the primary antibodies was done via a horseradish peroxidase-conjugated secondary antibody (anti-mouse 1:1000 and anti-rabbit 1:1000, Cell Signalling Technology, Frankfurt, Germany). Visualization was performed via Clarity Western ECL substrate (Bio-Rad Laboratories GmbH, Munich, Germany).

4.4 | Immunohistological staining

For histological investigations, the tissue was carefully washed after removal and pinned on cork plates to avoid curling during fixation in 4% paraformaldehyde.

After fixation for 24-48 hours, the tissue was dehydrated with ascending concentrations of ethanol according to the following protocol: 3x 70% (1 h), 1x 70% (overnight), 3x 80% (1 h), 1x 80% (overnight), 1x 90% (1 h), 2x 96% (1 h), 3x 99.5% (1 h); followed by ethanol: xylene (1:1, 40 min), 2x xylene (0.5 h), and liquid paraffin (overnight and 2x 1 h). Samples were then stored at room temperature until cutting (Leica RM 2245 microtome, Leica Microsystems, Heidelberg, Germany) and mounting. For deparaffinization, the slides were preheated for 1 hour at 56°C and then transferred to xylene at room temperature for 10 minutes. Afterwards the rehydration was performed by using descending alcohol series (>99.5%, 96%, 90%, 80%, 80%, deionized water) for 5 minutes each.

To expose the epitopes, the sections were incubated with 0.05% pronase in PBS for 10 minutes each at 37°C and then at room temperature, rinsed with 0.05% Tween20 in PBS (2x 2 min), and permeabilized with 0.5% Triton-X100 (5 min).

After washing (PBS, 2x 5 min), the sections were incubated (1 h) in blocking solution (5% Goat Serum + 1% BSA in PBS). The sections were then stained with the primary antibodies (rTRPV4 1:250, PA5-41066, ThermoFisher Scientific, Waltham, MA, USA and mTRPV3 1:500, ABIN863127, antibodies-online GmbH, Aachen, Germany) and stored at 4°C overnight. Each slide also carried a negative control, which was incubated with blocking solution only. The following day the slides were washed 5x 5 minutes with blocking solution and then incubated with the secondary antibody and 4′,6-diamidino-2-phenylindole (DAPI) in blocking solution (1:1000, Alexa Fluor 594 and 488, Thermo Fisher Scientific, Waltham, MA, USA) for 1 hour at 37°C in the dark. The slices were washed 5x 5 minutes with PBS, briefly rinsed in deionized water and ethanol and then embedded (ProTaqs Mount Fluor, Biocyc, Luckenwalde, Germany). The images were taken at 405, 488 and 543 nm using a confocal laser-scanning microscope (LSM 510, Axiovert200M, Zeiss, Jena, Germany).

4.4.1 | Analysis of digesta

For the analysis of ammonia and measurement of pH, the different segments of the gastrointestinal tract were clamped to avoid mixing of the digesta. After taking the sample, the pH value was immediately determined using a calibrated pH electrode and the sample was then frozen at −20°C until further analysis. The analysis of ammonia was determined by the Institute for Animal Nutrition of the FU Berlin by colorimetric determination.[83]

4.4.2 | Ussing chamber experiments

Tissues were removed about 10 minutes after the death of the animal, washed, stripped from the muscular layer and then transported with gassed (95% O_2 / 5% CO_2) ice-cooled transport buffer, which contained the following (in mmol·L^{-1}): 115 NaCl, 0.4 NaH_2PO_4, 2.4 Na_2HPO_4, 5 KCl, 25 $NaHCO_3$, 5 Glucose, 10 HEPES, 1.2 $CaCl_2$ and 1.2 $MgCl_2$ (pH 7.4).

The mucosal-submucosal preparations (stomach fundus, duodenum, middle jejunum, ileum, caecum or middle colon) were then mounted in 0.95 cm² Ussing chambers, initially filled with 10 mL NaCl-containing buffer solution per side at 37°C and gassed with either O_2 or carbogen (95% O_2/5% CO_2). All solutions were adjusted to 300 mosmol·kg^{-1} using mannitol. The measurements were performed in short-circuit mode; the transepithelial conductance G_t was continuously monitored via the potential response to a 100 µA current pulse (Mussler Scientific Instruments, Aachen, Germany). The mucosal bath was grounded and the sign convention is such that a positive I_{sc} reflects transport of cations from the mucosal to the serosal side. Recording commenced after a constant I_{sc} and G_t could be monitored or after 45 minutes at the latest.

In experiments that required a change in solution, the chamber liquid was drained off on both sides simultaneously and rapidly refilled with the test buffer on the mucosal side while the serosal side was refilled with the same standard serosal buffer as before. Both buffers were prewarmed and pregassed. In addition, some screening experiments were carried out in a small vertical Ussing chamber designed to allow continuous perfusion, thus minimizing artefacts because of solution changes.[14] For the composition of the solutions, see Supporting Tables B and C. For low chloride Ringer, NaCl, NMDGCl and NH_4Cl in Supporting Table C were replaced by Na-gluconate, NMDG-gluconate and NH_4-gluconate (generated via titration).

Stock solutions of the TRP channel modulators GSK106790A[70] and 2-APB[51] were prepared by dilution in ethanol and stored at −20°C and added directly to the mucosal bath (Supporting Table B) at 1:1000 yielding final concentrations of 100 µmol·L^{-1} (GSK106790A) and 1 mmol·L^{-1} (2-APB). Equivalent amounts of ethanol were added to the mucosal side of control tissues.

4.5 | Chemicals and modulators

Chemicals were purchased from Carl Roth (Karlsruhe, Germany), Sigma-Aldrich (Taufkirchen, Germany) or Merck (Darmstadt, Germany).

4.6 | Data and statistical analysis

Ussing chamber data were recorded at 10 points/min and binomially smoothed via Igor Pro 6.37 (WaveMetrics Inc, Lake Oswego, USA). Unless indicated otherwise, data were obtained 15 minutes after each intervention and tested for normal distribution (Shapiro–Wilk) and homogeneity of variance (Brown-Forsythe) using SigmaPlot 11.0 (Systat Software, Erkrath, Germany). Differences were evaluated with ANOVA or ANOVA on ranks using the Student-Newman-Keuls method. In some cases, the Dunn method was used, as suggested by SigmaPlot software. When comparing two groups, either the Student's *t*-test or the Mann-Whitney-U-test was performed.

Statistical analysis of the PCR results was performed with the resulting CNRQ values. Depending on the number of values to be compared, either a *t*-test or an ANOVA-test (two way, considering animal and respective localization of the tissue as factors) with a correction for multiple testing was applied.

The data are given as means ±SEM and the statistical significance was assumed if $P \leq .05$. The number of experiments is declared as N for the number of animals and n for the number of tissues.

ACKNOWLEDGEMENTS

This study was partly funded by a grant from the Akademie für Tiergesundheit (to DM). The antibodies and some other reagents were purchased with funding from Deutsche Forschungsgemeinschaft (DFG-STU 258/7-1). We would like to thank Prof. Dr Dorothee Günzel for the opportunity to produce the histological images and PD Dr Robert Pieper for the analysis of the intestinal ingesta. We would also like to thank Susanne Trappe, Martin Grunau and Katharina Söllig for their technical support.

CONFLICT OF INTEREST

This study was performed within a conventional academic setting for purely scientific reasons. At the time of the study, KTS and HSB were employees of PerformaNat GmbH, Germany, which also supplied some of the reagents for the study. Friederike Stumpff is not financially involved in Performanat in any way, but is the co-holder of patents EP2879662 (EU) and 9 693 971 (US) that were transferred to this start-up. There was no influence on the evaluation and interpretation of the data and there is no conflict of interest.

DATA AVAILABILITY STATEMENT

The data that support the findings of this study are available from the corresponding author upon reasonable request.

ORCID

David Manneck https://orcid.org/0000-0003-4478-1980
Hannah-Sophie Braun https://orcid.org/0000-0001-9293-7623
Katharina T. Schrapers https://orcid.org/0000-0003-0928-6394
Friederike Stumpff https://orcid.org/0000-0001-9518-9237

REFERENCES

1. Alaimo A, Rubert J. The pivotal role of TRP channels in homeostasis and diseases throughout the gastrointestinal tract. *Int J Mol Sci*. 2019;20(21):5277.
2. Holzer P. Transient receptor potential (TRP) channels as drug targets for diseases of the digestive system. *Pharmacol Ther*. 2011;131(1):142-170.
3. Montell C. The history of TRP channels, a commentary and reflection. *Pflugers Arch*. 2011;461(5):499-506.
4. Voets T, Droogmans G, Wissenbach U, Janssens A, Flockerzi V, Nilius B. The principle of temperature-dependent gating in cold- and heat-sensitive TRP channels. *Nature*. 2004;430(7001):748-754.
5. Vriens J, Nilius B, Vennekens R. Herbal compounds and toxins modulating TRP channels. *Curr Neuropharmacol*. 2008;6(1):79-96.
6. Diener M. Sensing osmolarity: a new player on the field. *J Physiol*. 2020;598(23):5297-5298.
7. Mergler S, Valtink M, Taetz K, et al. Characterization of transient receptor potential vanilloid channel 4 (TRPV4) in human corneal endothelial cells. *Exp Eye Res*. 2011;93(5):710-719.
8. Cseko K, Beckers B, Keszthelyi D, Helyes Z. Role of TRPV1 and TRPA1 ion channels in inflammatory bowel diseases: potential therapeutic targets? *Pharmaceuticals*. 2019;12(2):48.
9. Nozawa K, Kawabata-Shoda E, Doihara H, et al. TRPA1 regulates gastrointestinal motility through serotonin release from enterochromaffin cells. *Proc Natl Acad Sci U S A*. 2009;106(9):3408-3413.
10. Ueda T, Yamada T, Ugawa S, Ishida Y, Shimada S. TRPV3, a thermosensitive channel is expressed in mouse distal colon epithelium. *Biochem Biophys Res Commun*. 2009;383(1):130-134.
11. Kaji I, Yasuoka Y, Karaki S, Kuwahara A. Activation of TRPA1 by luminal stimuli induces EP4-mediated anion secretion in human and rat colon. *Am J Physiol Gastrointest Liver Physiol*. 2012;302(7):G690-G701.
12. Manneck D, Manz G, Braun H-S, Rosendahl J, Stumpff F. The TRPA1 agonist cinnamaldehyde induces the secretion of HCO3− by the porcine colon. *Int J Mol Sci*. 2021;22(10):5198.
13. Dimke H, Hoenderop JG, Bindels RJ. Molecular basis of epithelial Ca^{2+} and Mg^{2+} transport: insights from the TRP channel family. *J Physiol*. 2011;589(Pt 7):1535-1542.
14. Rosendahl J, Braun HS, Schrapers KT, Martens H, Stumpff F. Evidence for the functional involvement of members of the TRP channel family in the uptake of Na(+) and NH4 (+) by the ruminal epithelium. *Pflugers Arch*. 2016;468(8):1333-1352.
15. Wilkens MR, Kunert-Keil C, Brinkmeier H, Schröder B. Expression of calcium channel TRPV6 in ovine epithelial tissue. *Vet J*. 2009;182(2):294-300.
16. Schröder B, Breves G. Mechanisms and regulation of calcium absorption from the gastrointestinal tract in pigs and ruminants: comparative aspects with special emphasis on hypocalcemia in dairy cows. *Anim Health Res Rev*. 2006;7(1–2):31-41.
17. Wilkens MR, Muscher-Banse AS. Review: regulation of gastrointestinal and renal transport of calcium and phosphorus in ruminants. *Animal*. 2020;14(S1):s29-s43.
18. Martens H, Hammer U. Magnesium and sodium absorption from the isolated sheep rumen during intravenous aldosterone infusion (author's transl). *Dtsch Tierarztl Wochenschr*. 1981;88(10):404-407.
19. Martens H, Gabel G, Strozyk B. Mechanism of electrically silent Na and Cl transport across the rumen epithelium of sheep. *Exp Physiol*. 1991;76(1):103-114.
20. Sellin JH, Dubinsky WP. Apical nonspecific cation conductances in rabbit cecum. *Am J Physiol*. 1994;266(3 Pt 1):G475-G484.
21. Pouokam E, Diener M. Segmental differences in ion transport in rat cecum. *Pflugers Arch*. 2019;471(7):1007-1023.
22. Krattenmacher R, Voigt R, Clauss W. Ca-sensitive sodium absorption in the colon of Xenopus laevis. *J Comp Physiol B*. 1990;160(2):161-165.
23. Schultheiss G, Martens H. Ca-sensitive Na transport in sheep omasum. *Am J Physiol*. 1999;276(6 Pt 1):G1331-G1344.
24. Leonhard-Marek S, Stumpff F, Brinkmann I, Breves G, Martens H. Basolateral Mg2+/Na+ exchange regulates apical nonselective cation channel in sheep rumen epithelium via cytosolic Mg2+. *Am J Physiol Gastrointest Liver Physiol*. 2005;288(4):G630-G645.
25. Leonhard-Marek S. Divalent cations reduce the electrogenic transport of monovalent cations across rumen epithelium. *J Comp Physiol B*. 2002;172(7):635-641.
26. Voets T, Prenen J, Vriens J, et al. Molecular determinants of permeation through the cation channel TRPV4. *J Biol Chem*. 2002;277(37):33704-33710.
27. Owsianik G, Talavera K, Voets T, Nilius B. Permeation and selectivity of TRP channels. *Annu Rev Physiol*. 2006;68:685-717.

28. Bouron A, Kiselyov K, Oberwinkler J. Permeation, regulation and control of expression of TRP channels by trace metal ions. *Pflugers Arch*. 2015;467(6):1143-1164.
29. Schrapers KT, Sponder G, Liebe F, Liebe H, Stumpff F. The bovine TRPV3 as a pathway for the uptake of Na^+, Ca^{2+}, and NH^{4+}. *PLoS One*. 2018;13(3):e0193519.
30. Liebe F, Liebe H, Kaessmeyer S, Sponder G, Stumpff F. The TRPV3 channel of the bovine rumen: localization and functional characterization of a protein relevant for ruminal ammonia transport. *Pflugers Arch*. 2020;472(6):693-710.
31. Abdoun K, Stumpff F, Martens H. Ammonia and urea transport across the rumen epithelium: a review. *Anim Health Res Rev*. 2006;7(1-2):43-59.
32. Gerber PJ, Hristov AN, Henderson B, et al. Technical options for the mitigation of direct methane and nitrous oxide emissions from livestock: a review. *Animal*. 2013;7(Suppl. 2):220-234.
33. Mardini H, Record C. Pathogenesis of hepatic encephalopathy: lessons from nitrogen challenges in man. *Metab Brain Dis*. 2013;28(2):201-207.
34. Al-Awqati Q. One hundred years of membrane permeability: does Overton still rule? *Nat Cell Biol*. 1999;1(8):E201-E202.
35. Handlogten ME, Hong S-P, Zhang LI, et al. Expression of the ammonia transporter proteins Rh B glycoprotein and Rh C glycoprotein in the intestinal tract. *Am J Physiol Gastrointest Liver Physiol*. 2005;288(5):G1036-G1047.
36. Boron WF. Sharpey-Schafer lecture: gas channels. *Exp Physiol*. 2010;95(12):1107-1130.
37. Neuhäuser B, Dynowski M, Ludewig U. Switching substrate specificity of AMT/MEP/ Rh proteins. *Channels*. 2014;8(6):496-502.
38. Baday S, Orabi EA, Wang S, Lamoureux G, Bernèche S. Mechanism of NH4(+) recruitment and NH3 transport in Rh proteins. *Structure*. 2015;23(8):1550-1557.
39. Chepilko S, Zhou H, Sackin H, Palmer LG. Permeation and gating properties of a cloned renal K+ channel. *Am J Physiol*. 1995;268(2 Pt 1):C389-C401.
40. Burckhardt BC, Frömter E. Pathways of NH3/NH4+ permeation across Xenopus laevis oocyte cell membrane. *Pflugers Arch*. 1992;420(1):83-86.
41. Stumpff F, Lodemann U, Van Kessel AG, et al. Effects of dietary fibre and protein on urea transport across the cecal mucosa of piglets. *J Comp Physiol B*. 2013;183:1053-1063.
42. Szöllősi AG, Vasas N, Angyal Á, et al. Activation of TRPV3 regulates inflammatory actions of human epidermal keratinocytes. *J Invest Dermatol*. 2018;138(2):365-374.
43. Bergman EN. Energy contributions of volatile fatty acids from the gastrointestinal tract in various species. *Physiol Rev*. 1990;70(2):567-590.
44. Tappeiner H. Untersuchung über die Gärung der Cellulose, insbesondere über deren Lösung im Darmkanale. *Zeitschr f Biol*. 1884;20:52-134.
45. Gonzalez-Mariscal L, Contreras RG, Bolivar JJ, Ponce A, Chavez De Ramirez B, Cereijido M. Role of calcium in tight junction formation between epithelial cells. *Am J Physiol*. 1990;259(6 Pt 1):C978-C986.
46. Van Driessche W, Zeiske W. Ca^{2+}-sensitive, spontaneously fluctuating, cation channels in the apical membrane of the adult frog skin epithelium. *Pflugers Arch*. 1985;405(3):250-259.
47. Van Driessche W, Desmedt L, Simaels J. Blockage of Na^+ currents through poorly selective cation channels in the apical membrane of frog skin and toad urinary bladder. *Pflugers Arch*. 1991;418(3):193-203.
48. Cao X, Yang F, Zheng J, Wang K. Intracellular proton-mediated activation of TRPV3 channels accounts for the exfoliation effect of alpha-hydroxyl acids on keratinocytes. *J Biol Chem*. 2012;287(31):25905-25916.
49. Meoli L, Günzel D. Channel functions of claudins in the organization of biological systems. *Biochim Biophys Acta Biomembr*. 2020;1862(9):183344.
50. Bischof M, Olthoff S, Glas C, Thorn-Seshold O, Schaefer M, Hill K. TRPV3 endogenously expressed in murine colonic epithelial cells is inhibited by the novel TRPV3 blocker 26E01. *Cell Calcium*. 2020;92:102310.
51. Hu H-Z, Gu Q, Wang C, et al. 2-aminoethoxydiphenyl borate is a common activator of TRPV1, TRPV2, and TRPV3. *J Biol Chem*. 2004;279(34):35741-35748.
52. Hinman A, Chuang HH, Bautista DM, Julius D. TRP channel activation by reversible covalent modification. *Proc Natl Acad Sci U S A*. 2006;103(51):19564-19568.
53. Clapham DE. SnapShot: mammalian TRP channels. *Cell*. 2007;129(1):220.
54. Talavera K, Startek JB, Alvarez-Collazo J, et al. Mammalian transient receptor potential TRPA1 channels: from structure to disease. *Physiol Rev*. 2020;100(2):725-803.
55. Ma X, Nilius B, Wong JW, Huang Y, Yao X. Electrophysiological properties of heteromeric TRPV4-C1 channels. *Biochim Biophys Acta*. 2011;1808(12):2789-2797.
56. Huang Y-Y, Li J, Zhang H-R, et al. The effect of transient receptor potential vanilloid 4 on the intestinal epithelial barrier and human colonic cells was affected by tyrosine-phosphorylated claudin-7. *Biomed Pharmacother*. 2020;122:109697.
57. Martínez-Rendón J, Sánchez-Guzmán E, Rueda A, et al. TRPV4 regulates tight junctions and affects differentiation in a cell culture model of the corneal epithelium. *J Cell Physiol*. 2017;232(7):1794-1807.
58. Nijenhuis T, Hoenderop JG, Bindels RJ. TRPV5 and TRPV6 in Ca(2+) (re)absorption: regulating Ca(2+) entry at the gate. *Pflugers Arch*. 2005;451(1):181-192.
59. Schuchardt JP, Hahn A. Intestinal absorption and factors influencing bioavailability of magnesium-an update. *Curr Nutr Food Sci*. 2017;13(4):260-278.
60. Schlingmann KP, Weber S, Peters M, et al. Hypomagnesemia with secondary hypocalcemia is caused by mutations in TRPM6, a new member of the TRPM gene family. *Nat Genet*. 2002;31(2):166-170.
61. Rondón LJ, Groenestege WMT, Rayssiguier Y, Mazur A. Relationship between low magnesium status and TRPM6 expression in the kidney and large intestine. *Am J Physiol Regul Integr Comp Physiol*. 2008;294(6):R2001-R2007.
62. Holzer P. TRP channels in the digestive system. *Curr Pharm Biotechnol*. 2011;12(1):24-34.
63. Zou ZG, Rios FJ, Montezano AC, Touyz RM. TRPM7, magnesium, and signaling. *Int J Mol Sci*. 2019;20(8):1877.
64. Janssens A, Gees M, Toth BI, et al. Definition of two agonist types at the mammalian cold-activated channel TRPM8. *eLife*. 2016;5:e17240.
65. Fonfria E, Murdock PR, Cusdin FS, Benham CD, Kelsell RE, McNulty S. Tissue distribution profiles of the human TRPM cation channel family. *J Recept Signal Transduct Res*. 2006;26(3):159-178.
66. Amato A, Terzo S, Lentini L, Marchesa P, Mulè F. TRPM8 channel activation reduces the spontaneous contractions in human distal colon. *Int J Mol Sci*. 2020;21(15):5403.
67. Matsumoto K, Kurosawa E, Terui H, et al. Localization of TRPV1 and contractile effect of capsaicin in mouse large intestine: high

abundance and sensitivity in rectum and distal colon. *Am J Physiol Gastrointest Liver Physiol*. 2009;297(2):G348-360.
68. Rizopoulos T, Papadaki-Petrou H, Assimakopoulou M. Expression profiling of the Transient Receptor Potential Vanilloid (TRPV) channels 1, 2, 3 and 4 in mucosal epithelium of human ulcerative colitis. *Cells*. 2018;7(6):61.
69. Kun J, Szitter I, Kemény Á, et al. Upregulation of the transient receptor potential ankyrin 1 ion channel in the inflamed human and mouse colon and its protective roles. *PLoS One*. 2014;9(9):e108164.
70. Mihara H, Suzuki N, Boudaka AA, et al. Transient receptor potential vanilloid 4-dependent calcium influx and ATP release in mouse and rat gastric epithelia. *World J Gastroenterol*. 2016;22(24):5512-5519.
71. Kollmann P, Elfers K, Maurer S, Klingenspor M, Schemann M, Mazzuoli-Weber G. Submucosal enteric neurons of the cavine distal colon are sensitive to hypoosmolar stimuli. *J Physiol*. 2020;598(23):5317-5332.
72. Toledo Mauriño JJ, Fonseca-Camarillo G, Furuzawa-Carballeda J, et al. TRPV Subfamily (TRPV2, TRPV3, TRPV4, TRPV5, and TRPV6) gene and protein expression in patients with ulcerative colitis. *J Immunol Res*. 2020;2020:2906845.
73. Pritschow BW, Lange T, Kasch J, Kunert-Keil C, Liedtke W, Brinkmeier H. Functional TRPV4 channels are expressed in mouse skeletal muscle and can modulate resting Ca2+ influx and muscle fatigue. *Pflugers Arch*. 2011;461(1):115-122.
74. Hartmannsgruber V, Heyken W-T, Kacik M, et al. Arterial response to shear stress critically depends on endothelial TRPV4 expression. *PLoS One*. 2007;2(9):e827.
75. Xu H, Delling M, Jun JC, Clapham DE. Oregano, thyme and clove-derived flavors and skin sensitizers activate specific TRP channels. *Nat Neurosci*. 2006;9(5):628-635.
76. Ortar G, Morera L, Schiano Moriello A, et al. Modulation of thermo-transient receptor potential (thermo-TRP) channels by thymol-based compounds. *Bioorg Med Chem Lett*. 2012;22(10):3535-3539.
77. Nilius B, Biro T, Owsianik G. TRPV3: time to decipher a poorly understood family member! *J Physiol*. 2014;592(Pt 2):295-304.
78. Greco C, Leclerc-Mercier S, Chaumon S, et al. Use of epidermal growth factor receptor inhibitor erlotinib to treat palmoplantar keratoderma in patients with olmsted syndrome caused by TRPV3 mutations. *JAMA Dermatol*. 2020;156(2):191-195.
79. Peier AM, Reeve AJ, Andersson DA, et al. A heat-sensitive TRP channel expressed in keratinocytes. *Science*. 2002;296(5575):2046-2049.
80. Weiner ID, Verlander JW. Recent advances in understanding renal ammonia metabolism and transport. *Curr Opin Nephrol Hypertens*. 2016;25(5):436-443.
81. Stumpff F. A look at the smelly side of physiology: transport of short chain fatty acids. *Pflugers Arch*. 2018;470(4):571-598.
82. Braun HS, Sponder G, Pieper R, Aschenbach JR, Deiner C. GABA selectively increases mucin-1 expression in isolated pig jejunum. *Genes Nutr*. 2015;10(6):47.
83. Pieper R, Vahjen W, Neumann K, Van Kessel AG, Zentek J. Dose-dependent effects of dietary zinc oxide on bacterial communities and metabolic profiles in the ileum of weaned pigs. *J Anim Physiol Anim Nutr (Berl)*. 2012;96(5):825-833.

SUPPORTING INFORMATION

Additional Supporting Information may be found online in the Supporting Information section.

How to cite this article: Manneck D, Braun H-S, Schrapers KT, Stumpff F. TRPV3 and TRPV4 as candidate proteins for intestinal ammonium absorption. *Acta Physiol*. 2021;233:e13694. https://doi.org/10.1111/apha.13694